

See discussions, stats, and author profiles for this publication at: <https://www.researchgate.net/publication/263954840>

# Phase Equilibria of CO<sub>2</sub> + n-Alkane Binary Systems in Wide Ranges of Conditions: Development of Predictive Correlations Based on Cubic Mixing Rules

ARTICLE in INDUSTRIAL & ENGINEERING CHEMISTRY RESEARCH · APRIL 2012

Impact Factor: 2.59 · DOI: 10.1021/ie2018806

CITATIONS

12

READS

23

## 4 AUTHORS:



[Martín Cismondi](#)

National Scientific and Technical Research Co...

34 PUBLICATIONS 301 CITATIONS

SEE PROFILE



[S. B. Rodriguez-Reartes](#)

Universidad Nacional del Sur

8 PUBLICATIONS 47 CITATIONS

SEE PROFILE



[Juan M. Milanesio](#)

National Scientific and Technical Research Co...

9 PUBLICATIONS 29 CITATIONS

SEE PROFILE



[Marcelo S. Zabaloy](#)

Planta Piloto de Ingeniería Química

52 PUBLICATIONS 450 CITATIONS

SEE PROFILE

# Phase Equilibria of CO<sub>2</sub> + *n*-Alkane Binary Systems in Wide Ranges of Conditions: Development of Predictive Correlations Based on Cubic Mixing Rules

Martín Cismondi,<sup>\*,†,‡</sup> Sabrina B. Rodríguez-Reartes,<sup>†</sup> Juan M. Milanesio,<sup>†</sup> and Marcelo S. Zabaloy<sup>\*,†</sup>

<sup>†</sup>Planta Piloto de Ingeniería Química, Universidad Nacional del Sur—CONICET, CC 717, Camino La Carrindanga Km. 7, (8000) Bahía Blanca, Argentina

<sup>‡</sup>IDTQ (Grupo Vinculado PLAPIQUI-CONICET), Facultad de Ciencias Exactas Físicas y Naturales, Universidad Nacional de Córdoba, Av. Velez Sarsfield 1611, Córdoba, Argentina

## S Supporting Information

**ABSTRACT:** The phase equilibria of binary CO<sub>2</sub> + *n*-alkane mixtures have been studied by an important number of authors, both experimentally and using different types of thermodynamic models. Modeling studies of the phase behavior of such highly nonideal systems have generally achieved only partially accurate results in the correlation of phase equilibrium data when considering wide ranges of temperature, pressure, and *n*-alkane molecular weight. In this study, a predictive correlation for the phase behavior of CO<sub>2</sub> + *n*-alkane systems, based on a three-parameter cubic equation of state (EOS), that is, the RK-PR EOS, coupled to cubic mixing rules (CMRs), is developed and tested. CMRs have been shown to be capable of an accurate correlation of the phase equilibria asymmetric CO<sub>2</sub> + *n*-alkane binary systems, in wide ranges of temperature and pressure, when using system-specific interaction parameters. For developing the predictive correlation a critical review of published experimental data for the series was carried out, covering a total of about 100 references. An important degree of inaccuracy or scatter is often found when comparing data sets from different laboratories, specially for the more asymmetric systems (CO<sub>2</sub> + a long chain *n*-alkane). Tables of references covering CO<sub>2</sub> + *n*-alkane systems from C1 to C36 are presented for different types of experimental data, including critical end points (CEPs), critical points, liquid–liquid–vapor (LLV) equilibrium, and isobaric (Txy), isothermal (Pxy), and isoplethic (PT) two-phase equilibrium data sets. Examples of disagreement between different sets of data are presented and discussed. In some cases, a decision concerning the identification of the set that should be regarded as the most reliable, can be based on the experimental method employed, on the purity of the *n*-alkane, and on the observation of other data for conditions, and/or systems in the series, which are close to those of the data set under scrutiny. Nevertheless, the availability of such information is not enough, in other cases, to assess the quality of a given data set, where we have either different data sets in disagreement or a unique set, for which we are in doubt about its accuracy. In such situation, a predictive correlation for the whole series of binary systems is helpful to make a decision on the possible level of reliability of a given phase equilibrium data set. The present study is useful both to make decisions on conflicts between contradictory phase equilibrium data sets and to predict the phase equilibria of binary systems that have no experimental information available in the literature.

## 1. INTRODUCTION

When considering phase equilibria in mixtures, one very important family of binary systems, both from the technological and academic points of view, is the CO<sub>2</sub> + *n*-alkane homologue series. The importance of this series, sometimes taken as a reference in the analysis of other nonalkane + CO<sub>2</sub> binary mixtures, is clear when considering, for example, CO<sub>2</sub> injection as a method for enhanced oil recovery, the recent approaches for CO<sub>2</sub> sequestration in depleted oil wells, and extractions and separations using supercritical CO<sub>2</sub> as solvent.<sup>1,2</sup> Carbon dioxide has a large quadrupole moment<sup>3</sup> while *n*-alkanes are nonpolar and may have a molecular weight much greater than that of CO<sub>2</sub>. Therefore, most of the binary systems within the CO<sub>2</sub> + *n*-alkane homologue series are highly asymmetric with regard to both molecular size and energetic interactions. This makes the correlation/prediction of the phase equilibria of the series, over wide ranges of conditions, very difficult. This is a yet not fully solved relevant problem of physical chemistry. Most of the available previous attempts to describe the phase

equilibria of CO<sub>2</sub> + *n*-alkane systems in wide ranges of conditions were not completely successful (more details are provided elsewhere<sup>4</sup>).

Models of the equation of state (EOS) type<sup>5</sup> are the proper choice for describing the fluid phase equilibria over a wide range of pressure. This is because EOSs explicitly account for the effect of density on the thermodynamic properties of pure fluids and mixtures. A standard approach is to couple to EOS type models, mixing rules quadratic with respect to mole fraction (QMRs).<sup>5</sup> QMRs are double summations in mole fraction that make it possible to compute mixture parameters from pure-compound and interaction parameters. QMRs lack the flexibility required to describe highly asymmetric systems such as most of the CO<sub>2</sub> + *n*-alkane systems. In contrast, cubic

**Received:** August 22, 2011

**Revised:** March 26, 2012

**Accepted:** April 2, 2012

**Published:** April 2, 2012

mixing rules (CMRs)<sup>6</sup> provide a much higher flexibility with respect to composition.<sup>4</sup>

In a recent work,<sup>4</sup> CMRs, used for both the attractive and the repulsive mixture parameters, together with temperature-dependent interaction parameters, within the RK-PR EoS,<sup>7</sup> made it possible to achieve the best simultaneous representation of critical lines and liquid–liquid–vapor (LLV) equilibria that, to our knowledge, has ever been reported for CO<sub>2</sub> + *n*-alkane systems showing phase behavior of type III,<sup>8</sup> irrespective to the modeling approach used, in the open literature. Besides, a very good representation of two-phase equilibrium compositions in wide ranges of temperature and pressure was achieved<sup>4</sup> for the system CO<sub>2</sub> + *n*-hexadecane. This system could be regarded as the one with more and better experimental data available.<sup>4</sup> Such results<sup>4</sup> were obtained by using interaction parameters specific of the particular binary system considered.

The present study is essentially a continuation of such work,<sup>4</sup> in the process aiming to achieve a unique correlation of *n*-alkane carbon number-dependent interaction parameters, valid for describing the phase equilibria of the whole CO<sub>2</sub> + *n*-alkane homologue series.

Such a correlation would be useful to provisionally resolve conflicts between experimental data sets from different laboratories and also to predict the phase equilibria for CO<sub>2</sub> + *n*-alkane systems with no experimental data available.

As a piece of work required for achieving the stated general goal, we carried out a review on the experimental phase equilibrium data available for the series of CO<sub>2</sub> + *n*-alkane binary systems. Such a review was necessary to define our input for the parameter optimization problem. The review in the present work encompasses a range of binary systems wider than those in our previous work.<sup>4</sup>

It is important to note that, in view of the scatter frequently found when comparing different sets of data, and of the complexity of the high pressure phase behavior considered, it is often quite difficult to identify trends regarding the effect of temperature, pressure, or *n*-alkane carbon number on mutual solubilities.

This situation points to the need for a predictive model, which should be continuous, provide qualitatively correct patterns and trends, and have a good quantitative performance.

The requirements of continuity and proper qualitative behavior are achievable by choosing EOS-type thermodynamic models, specially EOSs of the van der Waals family, which are cubic with respect to molar volume, such as the RK-PR EOS.<sup>7</sup> Achieving a good quantitative performance—not attainable with quadratic mixing rules (QMRs) according to accumulated experience—is the main objective of the present work and should be possible to fulfill based on cubic mixing rules (CMRs). For an updated discussion on the approaches that different authors have implemented for modeling the phase equilibria of the CO<sub>2</sub> + *n*-alkane series and on their results, the reader is referred to our previous work.<sup>4</sup>

## 2. EXPERIMENTAL DATA ON THE FLUID PHASE EQUILIBRIA OF CARBON DIOXIDE + *N*-ALKANE SYSTEMS

We performed a literature review that focused on the experimental fluid phase equilibria of binary carbon dioxide + *n*-alkane systems, where the *n*-alkane of the mixture is a linear chain molecule having 1 to 36 carbon atoms. Equilibria with the presence of solid phases have not been taken into account. The literature on the experimental phase behavior of the CO<sub>2</sub> + *n*-alkane

homologue series is vast. Although we have identified an important number of relevant contributions, it is unlikely that our final list in the present work is complete. Due to space limitations, the complete information about the performed literature review is available as Appendix A in the Supporting Information. There, the information on CO<sub>2</sub> + *n*-alkane fluid phase equilibria is arranged in Tables A1 to A6. A given table corresponds to a specific type of phase equilibrium information, according to the summary given in Table 1.

**Table 1. Description of Tables with Information on Literature Contributions on the Experimental Fluid Phase Equilibria of CO<sub>2</sub> + *n*-Alkane Binary Mixtures**

| table <sup>a</sup> | type of experimental info.                              |
|--------------------|---|
| A1                 | fluid–fluid critical end points (CEPs)                  |
| A2                 | data sets of critical points                            |
| A3                 | liquid–liquid–vapor (LLV) data sets                     |
| A4                 | isothermal fluid–fluid equilibrium data sets (Pxy sets) |
| A5                 | isobaric fluid–fluid equilibrium data sets (Txy sets)   |
| A6                 | isoplethic fluid–fluid equilibrium data sets            |

<sup>a</sup>Tables A1 to A6 are available as Supporting Information.

According to Fall and Luks,<sup>9</sup> binary systems formed by carbon dioxide and *n*-alkanes up to C6 exhibit a type I behavior, according to the classification proposed by Scott and van Konynenburg<sup>8</sup> for the fluid phase behavior of binary mixtures (actually, it could be argued that the fluid phase behavior of these systems corresponds to type II but with the LLV region and the upper critical end point (UCEP) subject to the interference of the more stable solid–fluid equilibria). This means that a liquid = vapor (L = V) critical locus extends from the critical point of the pure *n*-alkane to the critical point of pure carbon dioxide, and there are no critical end points (CEPs). The binary systems containing CO<sub>2</sub> and *n*-alkanes from C7 to C12 display a type II phase behavior.<sup>8</sup> In type II behavior, a critical locus extends between the critical points of the pure compounds, as in type I behavior, and another critical locus (liquid = liquid, L = L) appears, which finishes in an upper critical end point (UCEP). A liquid–liquid–vapor (LLV) locus goes from that UCEP to lower temperatures. The system formed by CO<sub>2</sub> and *n*-tridecane constitutes a “transition” from type II to type III<sup>8</sup> phase behavior in this homologue series, and it presents a type IV behavior. In type IV phase behavior, the UCEP, which signals the end of the L = L critical locus, is also present, as in type II behavior. However, the critical line that stems from the critical point of the heavy compound (i.e., the *n*-alkane) ends at a lower critical end point (LCEP), and another critical locus extends from the critical point of pure CO<sub>2</sub> to a second UCEP (these last two types of critical lines were denoted E and D respectively, by Cismonti and Michelsen<sup>10</sup>). A LLV locus connects the last two CEPs. Finally, as already pointed out, for example, by Fall and Luks,<sup>9</sup> binary mixtures made of CO<sub>2</sub> and *n*-alkanes, with CN (carbon number of the *n*-alkane) ≥ 14, show a type III phase behavior. In this type of behavior, a critical locus connects the critical point of pure CO<sub>2</sub> with an UCEP, while there exists another critical locus that originates at the critical point of the pure *n*-alkane and extends indefinitely to high pressures. This latter critical locus (denoted C by Cismonti and Michelsen<sup>10</sup>) may show local extrema in the pressure versus temperature plane. As the difference between the critical temperatures of pure carbon dioxide and the pure *n*-alkane increases, the asymmetry of the mixture rises up, and we observe

an evolution in the fluid phase behavior for this homologue series. This kind of evolution has also been observed for other homologue series.<sup>5</sup>

The length of Table A4 (in Supporting Information) clearly shows that isothermal two-phase equilibrium is the type of experimental data most frequently gathered and reported for the CO<sub>2</sub> + *n*-alkane series. Often, specially for the heavier *n*-alkanes, some important degree of scatter is observed when graphically comparing data sets at the same temperature from different literature sources. Moreover, even serious disagreements can be found, as illustrated in Figure 1 for CO<sub>2</sub> + *n*-hexadecane at 313.2 K.

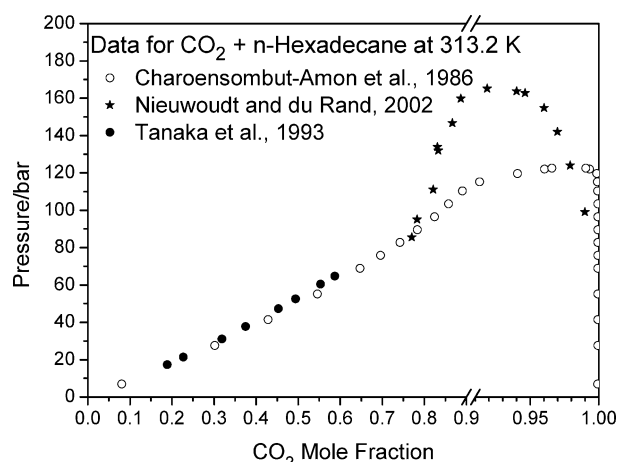


**Figure 1.** Experimental two-phase equilibrium data at 313.2 K for the CO<sub>2</sub> + *n*-hexadecane (C16) system. Markers: experimental data from a number of literature reports. This is an extreme example of disagreement between different sets of experimental data available in the literature. In this case, and considering other published data, such as some critical points, it seems that the data from Charoensombut-Amon et al. in the higher pressure range are wrong. Predictions for the same system and conditions are available in Figure 15A.

In this case, consideration of the critical line allows us to conclude that the data by Charoensombut-Amon et al.<sup>11</sup> at high pressures appear to be wrong. They suggest a false complete miscibility region, in a pressure range of about 50 bar, for mixtures that are actually globally unstable and separate into two phases. We observe that, even though the homologue series CO<sub>2</sub> + *n*-alkane has been widely studied, there is still some lack of important experimental information (see Table A3 in the Supporting Information).

### 3. MODELING APPROACH AND PARAMETERIZATION METHODOLOGY

Since this work is essentially a continuation of a previous one by Cismonti et al.,<sup>4</sup> the reader is referred to that work for a more detailed background on the approach followed to describe the fluid phase equilibria of CO<sub>2</sub> + *n*-alkane binary systems. That previous work<sup>4</sup> dealt with the procedure and results for the automated numerical optimization of the “binary system-specific” interaction parameters of CMRs + RK-PR EOS. The aim of such optimization<sup>4</sup> was to accurately reproduce the fluid phase behavior for all the CO<sub>2</sub> + *n*-alkane binary mixtures experimentally showing type III phase behavior, that is, those with *n*-alkane carbon numbers in the range from 14 to 22. The fundamental differences here with respect to that work<sup>4</sup> are two. First, now we consider not only type III phase behavior but all types of fluid phase behavior that take place in the CO<sub>2</sub> + *n*-alkane series, that is,

types I, II, IV, and III. Second, in addition to the individual optimization of a given system, we will consider a new and more ambitious objective function (OF). We have designed this OF to represent not the phase behavior of a specific CO<sub>2</sub> + *n*-alkane binary system but rather the behavior of the complete series of CO<sub>2</sub> + *n*-alkane binary mixtures—or an important part of it—as a whole. The reasons for considering a series-specific objective function are exposed in the following paragraphs.

Although the behavior of CO<sub>2</sub> + *n*-alkane binary mixtures for the lighter *n*-alkanes (type I) can generally be properly described with quadratic mixing rules (using  $k_{ij}$  and  $l_{ij}$  interaction parameters), it would, of course, be important also to consider such type I systems together with the “more difficult” asymmetric systems in the proposition and development of a more complex comprehensive approach for the series. In other words, in this work we describe all CO<sub>2</sub> + *n*-alkane binary mixtures using CMRs regardless the molecular weight of the *n*-alkane. On one hand, it is important that the mathematical formalism be unique for all binary systems in the series. Such unique mathematical formalism would be a requirement for dealing with multicomponent mixtures<sup>6</sup> (not considered in this work). On the other hand, since QMRs are a particular case of CMRs, available two-index interaction parameters for QMRs can be easily converted into equivalent three-index interaction parameters for CMRs. This conversion can be done by applying the relationships available in ref 6.

CMRs<sup>4</sup> provide eight binary interaction parameters if the repulsive ones are kept constant and the attractive ones are allowed to depend on temperature. Although CMRs provide us with great flexibility to model the phase behavior of complex systems through equations of state, we learned from our experience that it can be dangerous to free the eight CMRs interaction parameters while fitting them for a given binary system, if we do not have enough experimental information.

This can be due to the unbalanced uncertainty in the limited number of experimental data used in the objective function, and also in aiming to reproduce simultaneously two different types of phase behavior data, by using in the objective function experimental data from both the critical and classical regions.

In other words, even if we had hypothetically perfect experimental information, without error, the incompleteness or the unbalance in the set of data points used in the objective function could lead to an improper use of the CMRs flexibility, that is, to a poor prediction of regions not represented in the objective function while forcing a good reproduction of the covered ones. Our hypothesis is that, even without a crossover approach implemented, the CMRs’ flexibility can lead to a good description of both the classical and the critical regions simultaneously, provided that a careful and complete balance of data points is achieved within the objective function. When this condition is met, a proper trade-off takes place between the need for a good description of the phase equilibria in the classical region and that in the critical region, in parallel to a statistic neutralization of the uncertainty present in the data points. The latter assumes that inclusion of points with large systematic experimental errors has been prevented, and this is why a careful selection of data for the objective function is crucial. This hypothesis has been indeed confirmed in our previous work, at least for the case of CO<sub>2</sub> + *n*-hexadecane.<sup>4</sup>

However, the proper trade-off referred above is not easy to achieve, and we are limited by the availability of experimental phase equilibrium data for each particular binary CO<sub>2</sub> + *n*-alkane system. One alternative that we followed in some cases before,<sup>4</sup>



applicable to a binary system in the homologue series with some unavailable key experimental information, is to artificially generate pseudo-data points through interpolation between data for other homologue binary systems. Examples of key experimental information are some LLV equilibrium points or some critical end points. The generation of pseudo-data points is not straightforward and introduces extra sources of error in the parameter optimization process. Therefore, it may be regarded as questionable.

For all these reasons, the new alternative that we propose is to pursue the definition of a balanced objective function not for each system individually, but for the  $\text{CO}_2 + n$ -alkane series as a whole, and to adjust parameters that set the dependence of CMRs interaction parameters on the carbon number of the  $n$ -alkane rather than interaction parameters for individual binary systems. Such an approach has the added potential benefit of achieving predictive capability for those binary systems in the  $\text{CO}_2 + n$ -alkane series with limited or no experimental information available. This is partially the reason for our use of the words “predictive correlations” in the title of the present work. The proposed approach rests on the assumption of continuity for the phase behavior of different binary  $\text{CO}_2 + n$ -alkane systems along the series.

Attempts to correlate the phase equilibria of a homologue series rather than those of individual binary systems are not frequently found in the literature. An exception is some group contribution approaches, which have results of limited applicability in terms of temperature, pressure, and chain length ranges. An important and original work, in our opinion, was the one by Polishuk et al.,<sup>3</sup> which was based on carefully designed functionalities for the  $l_{ij}$  and temperature-dependent  $k_{ij}$  parameters in terms of pure compound covolumes and critical temperatures. In that work,<sup>3</sup> the authors managed to obtain a quite good representation of the general behavior for the series  $\text{CO}_2 + n$ -alkanes. This was done<sup>3</sup> by matching only three experimental key-points, aimed to provide the appropriate balance between liquid–liquid equilibrium (LLE) and liquid–vapor equilibrium (LVE) behavior. The limitations in those results were mainly in the quantitative description of liquid phases either at LVE or, specially, at liquid–liquid–vapor equilibrium (LLVE) in the lower temperature range and in the quantitative description of the liquid–liquid critical lines toward high pressures. In the present work, given the higher flexibility of CMRs and the corresponding goal of achieving a better quantitative performance, it was necessary to consider different types of experimental data and to choose a proper objective function, as it is discussed in section 3.2

**3.1. Equation of State, Mixing Rules, and Pure Compound Parameters.** As in our previous work,<sup>4</sup> we use here the RK-PR EOS<sup>7</sup> and cubic mixing rules (CMRs).<sup>6</sup> CMRs are the following:

$$a = \sum_{i=1}^N \sum_{j=1}^N \sum_{k=1}^N x_i x_j x_k a_{ijk} \quad (1)$$

$$a_{ijk} = (a_i a_j a_k)^{(1/3)} (1 - k_{ijk}) \quad (2)$$

$$b = \sum_{i=1}^N \sum_{j=1}^N \sum_{k=1}^N x_i x_j x_k b_{ijk} \quad (3)$$

$$b_{ijk} = \left( \frac{b_i + b_j + b_k}{3} \right) (1 - l_{ijk}) \quad (4)$$

where  $N$  is the number of components in a multicomponent mixture,  $a_i$ ,  $b_i$ , and  $x_i$  are, for component  $i$ , the attractive energy parameter, the repulsive covolume parameter, and the mole fraction in the system, respectively,  $k_{ijk}$  and  $l_{ijk}$  are respectively the attractive energy interaction parameter and the covolume interaction parameter. For a binary system of components 1 and 2, the cubic mixing rules provide four independent interaction parameters:  $k_{112}$ ,  $k_{122}$ ,  $l_{112}$ , and  $l_{122}$ .

It is generally accepted that the properties of a dense, highly nonideal binary mixture made of two given types of molecules (e.g. molecules A and B) depend strongly on the relative amounts of components A and B, specially when comparing the extreme situations where component A is infinitely diluted in component B and, at the opposite end, where component B is infinitely diluted in component A. It can be shown for CMRs<sup>6</sup> that the partial molar properties for component 1, when component 1 is infinitely diluted in component 2, depend on  $k_{122}$  and  $l_{122}$  but not on  $k_{112}$  and  $l_{112}$ . Analogously, the partial molar properties for component 2, when component 2 is infinitely diluted in component 1, depend on  $k_{112}$  and  $l_{112}$  but not on  $k_{122}$  and  $l_{122}$ .<sup>6</sup> Thus, CMRs provide the means for controlling independently the properties of the fluid binary mixture at the two infinite dilution limits. This is needed, for instance, for a proper description of liquid–liquid equilibria of highly asymmetric mixtures. Notice that at any temperature and composition the mixture parameters  $a$  and  $b$  must be positive.

The attractive energy interaction parameters are made temperature-dependent as follows:<sup>4</sup>

$$k_{ijk} = k_{ijk}^{\infty} + k'_{ijk} e^{-T/T_{ijk}^*} \quad (5)$$

From eq 5,  $k_{ijk}$  is a monotonically decreasing or increasing function of temperature  $T$ , depending on the sign of  $k'_{ijk}$ . Parameter  $k_{ijk}$  asymptotically tends to  $k_{ijk}^{\infty}$  as temperature  $T$  tends to infinity. At  $T = 0$ , parameter  $k_{ijk}$  has a finite value equal to  $k_{ijk}^0 = (k_{ijk}^{\infty} + k'_{ijk})$ . The rate at which the transition from  $k_{ijk}^0$  to  $k_{ijk}^{\infty}$  takes place is controlled by parameter  $T_{ijk}^*$ . The total number of available independent CMRs binary interaction parameters is eight:  $l_{112}$ ,  $k_{112}^{\infty}$ ,  $k'_{112}$ ,  $T_{112}^*$ ,  $l_{122}$ ,  $k_{122}^{\infty}$ ,  $k'_{122}$ , and  $T_{122}^*$ . Polishuk has used CMRs but in a form that cannot be extended to multicomponent mixtures.<sup>12</sup>

Regarding the pure compound parameters of the RK-PR EOS,<sup>7</sup> we have made a choice different than in previous works. Based on previous observations, and with the goal of improving the prediction of densities, we decided to match the saturated liquid density of carbon dioxide at 270 K. Also, in order to get a more regular evolution of the pure  $n$ -alkane parameters than that obtained in our previous work,<sup>4</sup> which was influenced by triple point temperatures, now the experimental saturated liquid volume is reproduced at a reduced temperature of 0.7 for all the  $n$ -alkanes. The resulting pure compound parameters used in this work are given in Table B1 in the Supporting Information. Notice that Table B1 also provides short acronyms for the compounds, for example, C5 for  $n$ -pentane.

The three-parameter RK-PR EoS<sup>7</sup> is the following:

$$P = \frac{RT}{v - b} - \frac{a}{(v + \delta_1 b) \left( v + \frac{1 - \delta_1}{1 + \delta_1} b \right)} \quad (6)$$

where

$$a_i(T) = a_{c,i} \left( \frac{3}{2 + T/T_{c,i}} \right)^{k_i} \quad (7)$$

$P$  is the absolute pressure,  $v$  the molar volume,  $R$  the universal gas constant,  $a_{c,i}$  the critical attractive energy parameter for pure compound  $i$ ,  $T_{c,i}$  the critical temperature of pure compound  $i$ , and  $k_i$  a pure compound parameter that influences the temperature dependence of the attractive energy parameter. A linear mixing rule is set for the third parameter  $\delta_1$ . See Table B1 in the Supporting Information.

**3.2. Objective Function and Experimental Data Selected.** With respect to the objective function, the differences and particularities that naturally arise when aiming at the optimization of CN-dependent interaction parameters of the CO<sub>2</sub> +  $n$ -alkane series, instead of aiming at the optimization of “binary system-specific” interaction parameters, are the following:

- (1) It is not necessary to consider experimental phase equilibrium points for all the binary systems of the homologue series, neither it is to include binary pseudoexperimental points, obtained by interpolation between experimental points of the same nature for other binary systems. Therefore, we will consider only selected experimental points.
- (2) If we set an  $n$ -degree polynomial dependence with respect to the carbon number (CN) of the  $n$ -alkane, for each CMRs interaction parameter, then, the number of free parameters in the optimization will equal  $(n + 1)$  times the number of CMRs' available independent interaction parameters; that is, it will equal  $[8(n + 1)]$ . Notice that, when considering the whole CO<sub>2</sub> +  $n$ -alkane series, it is reasonable to allow the  $T^*$  parameters of eq 5 to depend on CN (instead of keeping them constant, as we did for CN from 14 to 22 in our previous work<sup>4</sup>). The number of polynomial functions whose parameters are to be adjusted is eight.
- (3) When selecting the phase equilibrium experimental data, we need to achieve a balance in different aspects simultaneously: between different types of data points [liquid–vapor equilibrium (LVE), liquid–liquid equilibrium (LLE), critical points, etc.], covering the range of CN from the lightest to the heavier  $n$ -alkanes, and covering also wide ranges of temperature and pressure.

We tried different polynomial dependences with respect to CN for the interaction parameters. A quartic form, for example, can be set as follows:

$$p = a_p + b_p \text{CN} + c_p \text{CN}^2 + d_p \text{CN}^3 + e_p \text{CN}^4 \quad (8)$$

where

$$p = l_{112}, l_{122}, k'_{112}, k'_{122}, k_{112}^\infty, k_{122}^\infty, T_{112}^*, \text{ or } T_{122}^* \quad (9)$$

where parameters  $a_p$ ,  $b_p$ ,  $c_p$ ,  $d_p$ , and  $e_p$  are characteristic of the CO<sub>2</sub> +  $n$ -alkane homologue series, or at least of an important part of it.

See the next section for the final polynomial expression and constants for the eight parameters. The objective function used in this work is the following:

$$\text{OF} = \sum_{i=1}^{\text{NTP}} \frac{(\text{KP}_i^{\text{calc}} - \text{KP}_i^{\text{expt}})^2}{\text{KP}_i^{\text{expt}}} + \sum_{j=1}^{\text{Nz}} \left[ \left| \ln \left( \frac{z_{j,1}^{\text{calc}}}{z_{j,1}^{\text{expt}}} \right) \right| + \left| \ln \left( \frac{z_{j,2}^{\text{calc}}}{z_{j,2}^{\text{expt}}} \right) \right| \right] \quad (10)$$

where  $\text{KP}_i$  is either the temperature coordinate or the pressure coordinate of a binary phase equilibrium key point. The

superscript “expt” means “experimental value” while the superscript “calc” means “calculated value”.  $\text{KP}_i$  can be, for type III CO<sub>2</sub> +  $n$ -alkane systems, the following (see Figure 2 of ref 4 and Table 3 of the present work): the pressure coordinate of the local minimum of the binary critical curve ( $\text{CP}_m$ ), the minimum temperature in the liquid–liquid like part of the critical line ( $T_m$ ), the critical temperature at the maximum critical pressure experimentally available ( $\text{CT}_{994}$ ), or the critical pressure at the maximum critical temperature experimentally available ( $\text{CP}_{393.3}$ ).  $\text{KP}_i$  can also be a critical pressure ( $P_c$ , see Table 2) of a binary system, the temperature of a critical end

**Table 2. Experimental Liquid–Vapor Critical Pressures ( $P_c$ ) and Critical Compositions [ $z_c$  (CO<sub>2</sub>)] at Given Temperatures for Some CO<sub>2</sub> +  $n$ -Alkane Systems<sup>a</sup>**

| system                           | temp. (K) | $P_c$ (bar) | $z_c$ (CO <sub>2</sub> ) | ref                                  |
|----------------------------------|-----------|-------------|--------------------------|--------------------------------------|
| CO <sub>2</sub> + methane        | 219.3     | 64.68       | 0.252                    | Mraw et al., 1978 <sup>30</sup>      |
|                                  | 270.0     | 85.11       | 0.6468                   | Al-Sahhaf et al., 1983 <sup>31</sup> |
| CO <sub>2</sub> + ethane         | 296.82    | 53.52       | 0.2403                   | Horstmann et al., 2000 <sup>32</sup> |
| CO <sub>2</sub> + propane        | 327.0     | 65.2        | 0.60                     | Smejkal et al., 2002 <sup>33</sup>   |
| CO <sub>2</sub> + $n$ -butane    | 344.3     | 81.2        | 0.72                     | Hsu et al., 1985 <sup>34</sup>       |
| CO <sub>2</sub> + $n$ -hexane    | 387.0     | 117.2       | 0.78                     | Liu et al., 2003 <sup>35</sup>       |
| CO <sub>2</sub> + $n$ -octane    | 359.5     | 130.1       | 0.878                    | Choi and Yeo, 1998 <sup>36</sup>     |
| CO <sub>2</sub> + $n$ -decane    | 444.26    | 188.36      | 0.843                    | Reamer and Sage, 1963 <sup>37</sup>  |
|                                  | 577.04    | 78.6        | 0.40                     |                                      |
| CO <sub>2</sub> + $n$ -tridecane | 377.4     | 198.0       | 0.925                    | Enick et al., 1985 <sup>38</sup>     |

<sup>a</sup>Data selected as input for the objective function.

point or of a K point (Table 4), the saturation pressure at given temperature and composition (Table B3, Supporting Information), or the azeotropic pressure (only for the case of CO<sub>2</sub> + ethane).  $z_{j,1}$  and  $z_{j,2}$  are respectively the mole fractions of CO<sub>2</sub> (1) and of the  $n$ -alkane (2). These mole fractions can be the following: the critical composition (Table 2), the composition of a liquid phase under conditions of LLV equilibrium (Table 5), the composition of a phase under two-phase equilibrium conditions at given temperature and pressure (Table B2, Supporting Information), or the azeotropic composition (only for the case of CO<sub>2</sub> + ethane). NTP is the number of experimental pressure and temperature values used in the objective function. Analogously, Nz is the number of experimental mole fraction vectors used in the objective function.

The phase equilibrium points considered in the objective function can be classified in four main groups: critical points, critical end point temperatures, liquid–liquid–vapor equilibrium (LLVE), and two-phase equilibrium.

**Critical Points.** For some CO<sub>2</sub> +  $n$ -alkane systems with phase behavior of types I, II, and IV, we compute the pressure ( $P_c$ ) and composition ( $z_c$ ) of the liquid–vapor critical point at a selected temperature (Table 2), while for type III systems the same four characteristic critical coordinates previously defined<sup>4</sup> ( $\text{CT}_{994}$ ,  $T_m$ ,  $\text{CP}_m$ , and  $\text{CP}_{393.3}$ ) were considered (Table 3). Note in Table 2 that two critical points were considered only for the systems with methane and  $n$ -decane.

**Critical End Point Temperatures.** The upper critical end points (UCEPs) for the systems CO<sub>2</sub> + C8 and CO<sub>2</sub> + C10 (type II) were considered, as well as the three characteristic CEPs for the transition system CO<sub>2</sub> + C13 (type IV). The experimental CEP temperature values and references are given

**Table 3. Characteristic Experimental Critical Coordinates for Some Type III CO<sub>2</sub> + *n*-Alkane Systems, Selected for the Objective Function<sup>a</sup>**

| CN <sup>b</sup> | CT <sub>994</sub> <sup>c</sup><br>(K) | T <sub>m</sub> <sup>d</sup><br>(K) | CP <sub>m</sub> <sup>e</sup><br>(bar) | CP <sub>393.3</sub> <sup>f</sup> (bar) | ref  |
|-----------------|---------------------------------------|------------------------------------|---------------------------------------|--|--|
| 14              | 294.40                                | 283.1                              | 78                                    | 226.6                                  | Scheidgen <sup>39</sup>                          |
| 16              | 305.45                                | 297.6                              | 166                                   | 256                                    | Scheidgen Spee and Schneider, 1991 <sup>40</sup> |
| 19              | 321.51                                | 317.2                              | 269                                   | 304                                    | Scheidgen <sup>39</sup>                          |
| 22              | 335.97                                | 334.2                              | 350                                   | 357                                    | Scheidgen <sup>39</sup>                          |

<sup>a</sup>The pressures informed in the references range from 991 to 997.8 bar. The temperatures informed in the references range from 393.14 to 393.59 K. <sup>b</sup>CN: carbon number of the *n*-alkane. <sup>c</sup>CT<sub>994</sub>: critical temperature at 994 bar. <sup>d</sup>T<sub>m</sub>: minimum temperature in the liquid–liquid like part of the critical line. <sup>e</sup>CP<sub>m</sub>: pressure coordinate of the local minimum of the binary critical curve. <sup>f</sup>CT<sub>393.3</sub>: critical pressure at 393.3 K.

in Table 4. K points (which are liquid–vapor UCEPs) in CO<sub>2</sub> + *n*-alkane systems with phase behavior of type III were

**Table 4. Experimental Fluid–Fluid Critical End Point Temperatures for Some CO<sub>2</sub> + *n*-Alkane Systems, Considered in the Objective Function**

| CN | type | UCEP<br>temp.<br>(K) | LCEP<br>temp.<br>(K) | K point<br>temp. (K) | ref  |
|----|------|----------------------|----------------------|----------------------|--|
| 8  | II   | 231.5                |                      |                      | Hottovy et al., 1982 <sup>41</sup>                                       |
| 10 | II   | 248.7                |                      |                      | Kulkarni et al., 1974 <sup>42</sup>                                      |
| 13 | IV   | 279.0                | 310.8                | 314.0                | Hottovy et al., 1981, <sup>43</sup> and Fall and Luks, 1985 <sup>9</sup> |

not included, since their temperatures are much less sensitive to the interaction parameters, and experimentally less changing along the series, than for example the LL-UCEPs (see Figure 3).

**Liquid–Liquid–Vapor Equilibrium (LLVE).** The compositions of the liquid phases under conditions of LLVE, at a selected relatively low temperature, that is, away from the CEP, have been included for certain systems from CO<sub>2</sub> + C8 to CO<sub>2</sub> + C20 (Table 5).

**Table 5. Experimental Liquid–Liquid–Vapor (LLV) Equilibrium Key-Points for Some CO<sub>2</sub> + *n*-Alkane Binary Mixtures Considered in the Objective Function**

| CN | T <sub>lowLLV</sub><br>(K) | x <sub>lowLLV</sub> <sup>a</sup> | y <sub>lowLLV</sub> <sup>a</sup> | ref   |
|----|----------------------------|----------------------------------|----------------------------------|---|
| 8  | 216                        | 0.444                            | 0.978                            | Hottovy et al., 1982 <sup>41</sup>              |
| 10 | 238.15                     | 0.602                            | 0.970                            | Kulkarni et al., 1974 <sup>42</sup>             |
| 13 | 258.0                      | 0.650                            | 0.9815                           | Hottovy et al., 1981 <sup>43</sup>              |
| 14 | 270.0                      | 0.707                            | 0.9815                           | Hottovy et al., 1981 <sup>43</sup>              |
| 16 | 283.2                      | 0.716                            | 0.9868                           | van der Steen et al., 1989 <sup>44</sup>        |
| 19 | 292.9                      | 0.704                            | 0.9958                           | Fall et al., 1985 <sup>45</sup> (smoothed data) |
| 20 | 300.4                      | 0.704                            | 0.998                            | Huie et al., 1973 <sup>26</sup>                 |

<sup>a</sup>x<sub>lowLLV</sub> and y<sub>lowLLV</sub>: compositions (CO<sub>2</sub> mole fraction) of the two liquid phases, under LLV conditions, at a selected low temperature T<sub>lowLLV</sub>.

**Two-Phase Equilibrium.** Two different types of departures are computed in the objective function of eq 10 regarding two-phase equilibrium behavior: mainly composition departures for both phases at specified *T* and *P* (Table B2, Supporting

Information), but also bubble pressure departures at specified composition *x*<sub>1</sub> and *T* (Table B3, Supporting Information). Notice that the phase composition values in Table B2 (Supporting Information) indicate that methane (CN = 1) is lighter than CO<sub>2</sub> and that the system CO<sub>2</sub> + ethane (CN = 2) is azeotropic.

In addition, we included the azeotropic pressures and compositions for the system with ethane at 243.15 and 283.15 K, as reported by Fredenslund and Mollerup.<sup>13</sup>

In most cases, we selected the data either because there was good agreement between data sets from different laboratories, or because the data showed regular and smooth trends with respect to the *n*-alkane carbon number. This is, for example, the case of critical lines in type III CO<sub>2</sub> + *n*-alkane systems.

**3.3. Optimization Strategy.** As is usual in optimization processes, the problem of getting initial values for the parameters to optimize is important, and this is true especially in this case as a result of the high quantitative and qualitative sensitivity of the systems phase behavior to the parameters. Based on the arguments expressed in section 3, this is the new strategy we follow in the present work:

- Optimize the eight interaction parameters for each binary CO<sub>2</sub> + *n*-alkane system for which we have available relatively enough reliable information: we have considered here the binaries with C10, C13, C16, and C20. For each of these first individual optimizations (determination of 8 parameters per binary system), we used all the corresponding data in Tables 2–5 and Tables B2 and B3 in the Supporting Information, plus:
  - Artificial CT<sub>994</sub> values for C10 (269.2 K) and C13 (288.1 K), extrapolated from data in Table 3 (this work) or Table 2 in ref 4.
  - K point temperature and heavy phase composition values for C16 and C20 (Table 3 in ref 4), and also K point CO<sub>2</sub> molar fraction for C13 = 0.885 (taken from ref 9).
  - Artificial (CT<sub>994</sub>, T<sub>m</sub>, CP<sub>m</sub>, CP<sub>393.3</sub>) values for C20 (Table 2 in ref 4).
- Considering the values obtained for the eight interaction parameters for the first four systems (CO<sub>2</sub> + *n*-alkane systems with C10, C13, C16, and C20), identify the four interaction parameters whose values show the most regular behavior versus CN and perform a quadratic regression for each one.
- Optimize the CO<sub>2</sub> + *n*-alkane systems for which we have some important, but incomplete, experimental phase equilibrium information. In these cases, only four parameters will be free during the optimization process, while the other four (those identified in the previous point) will be fixed at predicted values from the quadratic regressions of the previous step. We considered at this stage the CO<sub>2</sub> + *n*-alkane binary systems with C3, C4, C6, C8, C14, C22, and C28 and also reconsidered the systems from point 1.
- From the values obtained for each interaction parameter in the previous step, make a parameter regression corresponding to a polynomial form of third order, for each interaction parameter as a function of CN.
- Taking the regression constants from steps 2 and 4 as the initial guess, optimize the third order polynomial

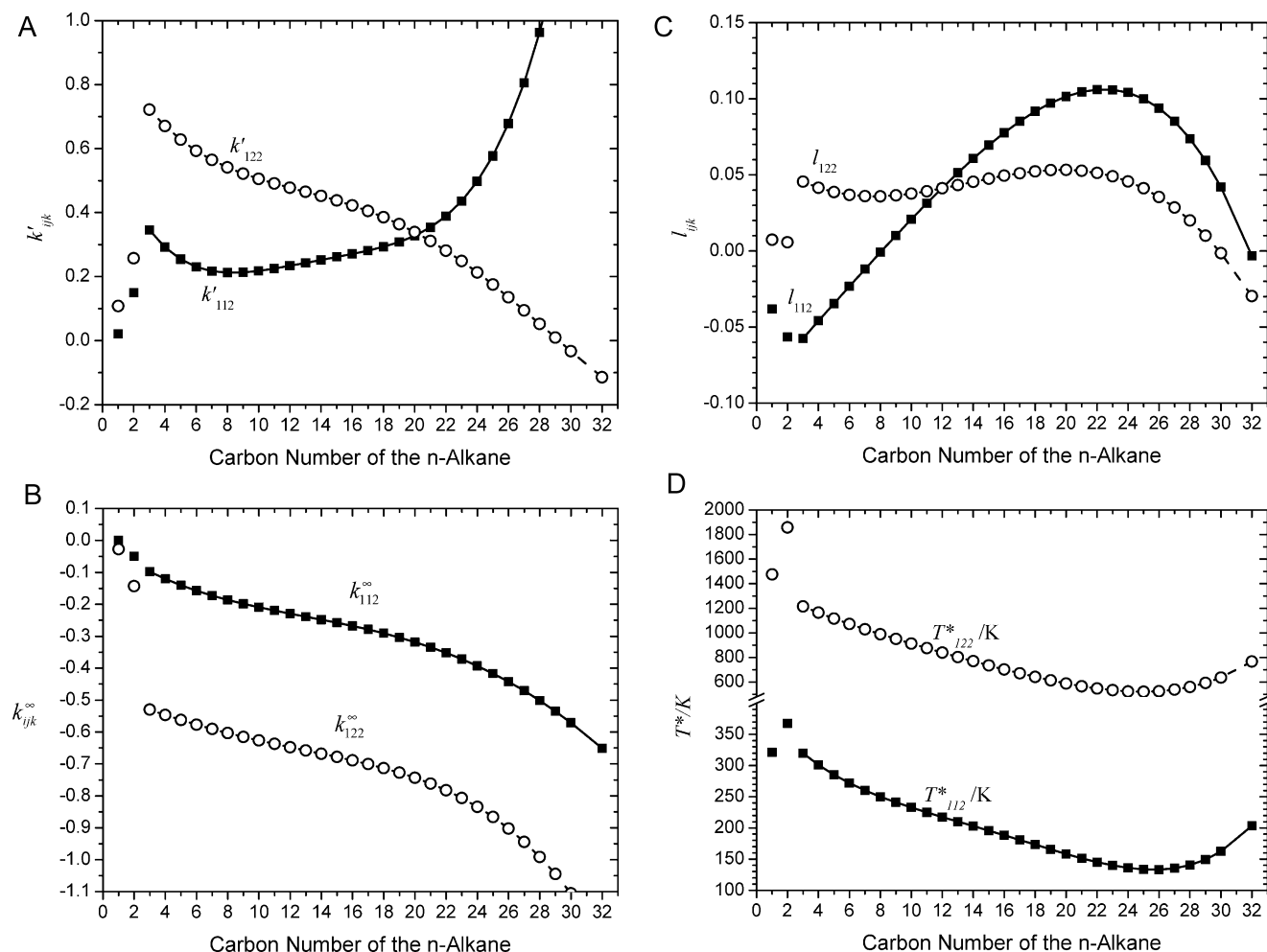


**Figure 2.** Evolution of the CMRs interaction parameters as functions of the *n*-alkane carbon number (CN) for the CO<sub>2</sub>(1) + *n*-alkane (2) homologue series. From CN = 3 to CN = 32 this evolution is given by the correlation, proposed for the homologue series, represented by eq 11 used with the parameter values of Table 6. The individually obtained interaction parameters for CO<sub>2</sub> + C1 and CO<sub>2</sub> + C2 (Table B4, Supporting Information) are also included in this figure. Model: RK-PR EOS with CMRs.

constants for the eight CMRs interaction parameters (and eventually fourth order if necessary), considering all the experimental data in Tables 2–5 and Tables B2 and B3 in the Supporting Information, and no other, so that artificial data do not influence the final parameters characteristic of the CO<sub>2</sub> + *n*-alkane homologue series.

We stress that in eq 10 we have used KP only for key-point temperature or pressure coordinates and *z* for key-point compositional coordinates. In comparison to the terms we used before<sup>4</sup> for defining the objective function, now the KP terms for temperature or pressure values are more weighted (note that these terms are not dimensionless anymore and that the values should be in K and bar, respectively). Also, in the key-point composition terms [*j*-summation in eq 10], the  $z_{j,l}^{\text{calc}}/z_{j,l}^{\text{expt}}$  ratios different from unity are now penalized rather than the differences ( $z_{j,l}^{\text{calc}} - z_{j,l}^{\text{expt}}$ ). This will assign enough importance to the experimental points in diluted regions, for example, to mixtures of compound 1 diluted in 2, whose equilibria are governed, when using CMRs, by the binary parameters with indices 1, 2, and 2, that is,  $l_{122}$ ,  $k^{\infty}_{122}$ ,  $k'_{122}$  and  $T^*_{122}$ .

For minimizing our objective functions with different numbers of systems and points, we used the FORTRAN

function Praxis, for unconstrained optimization. Praxis is based on the principal axis method by Richard Brent.<sup>14,15</sup>

We have evaluated (a) the results of a unique correlation for the whole series, that is, for the binary systems from CO<sub>2</sub> + C1 to CO<sub>2</sub> + C32 considered all together, and (b) the results of complementary runs carried out after removing from the objective function the terms corresponding to one or more specific binary systems. Such results showed that the partial objective functions for some binary systems could be further decreased but at the expense of increasing the partial objective function of other systems. By partial objective function, we mean the contribution by a specific binary CO<sub>2</sub> + *n*-alkane system to the objective function of the CO<sub>2</sub> + *n*-alkane homologue series. The removal of one or two of the heavier alkane CO<sub>2</sub> + *n*-alkane systems did not lead to a significant improvement for the rest of the series, but the result was different after eliminating the binary systems with the lightest *n*-alkanes, that is, the systems CO<sub>2</sub> + C1 and CO<sub>2</sub> + C2. Therefore, we finally decided to generate a correlation valid from C3 on, and to adjust the first two systems (CO<sub>2</sub> + C1 and CO<sub>2</sub> + C2) individually.

Although the correlation could be expressed exactly in the form of eq 8, we present the polynomial functions, and corresponding values for the coefficients, based on the independent variable



Table 6. Correlation Constants for the CMRs Interaction Parameters of the CO<sub>2</sub>(1) + *n*-Alkane (2) Homologue Series for *n*-Alkane Carbon Numbers from 3 to 32 (eq 11)<sup>a</sup>

| interaction param. |                      | param.   |          |          |           |            |
|--------------------|----------------------|----------|----------|----------|-----------|------------|
|                    |                      | $a_p$    | $10b_p$  | $100c_p$ | $1000d_p$ | $10000e_p$ |
| interaction param. | $k'_{112}$           | 0.24280  | 0.09265  | 0.00300  | −0.04749  | 0.14508    |
|                    | $k'_{122}$           | 0.46507  | −0.12826 | −0.01555 | −0.10831  | 0.03556    |
|                    | $k^{\infty}_{112}$   | −0.23865 | −0.09383 | −0.00099 | −0.04289  | 0.00487    |
|                    | $k^{\infty}_{122}$   | −0.65776 | −0.10049 | 0.00026  | −0.03794  | −0.01094   |
|                    | $l_{112}$            | 0.05138  | 0.09621  | −0.02287 | −0.01446  | −0.00428   |
|                    | $l_{122}$            | 0.04326  | 0.02134  | 0.00336  | −0.01963  | 0.00069    |
|                    | $T^*_{112}/1000$ (K) | 0.21033  | −0.07266 | 0.00047  | −0.01727  | 0.01903    |
|                    | $T^*_{122}/1000$ (K) | 0.80392  | −0.35007 | 0.03694  | 0.00913   | 0.03312    |
|                    |                      |          |          |          |           |            |
|                    |                      |          |          |          |           |            |

<sup>a</sup>Model: RKPR-EOS.

(CN-13) in accordance with the actual optimization procedure we followed:

$$p = a_p + b_p(\text{CN}-13) + c_p(\text{CN}-13)^2 + d_p(\text{CN}-13)^3 + e_p(\text{CN}-13)^4 \quad (11)$$

where  $p = l_{112}, l_{122}, k'_{112}, k'_{122}, k^{\infty}_{112}, k^{\infty}_{122}, T^*_{112}, T^*_{122}$ . Note that for a given interaction parameter  $p$  the constant  $a_p$  is the parameter value for the binary system CO<sub>2</sub> + *n*-tridecane. The interaction parameters obtained from these correlations are shown in Figure 2 as functions of CN. Figure 2 also shows the interaction parameters for the systems CO<sub>2</sub> + methane and CO<sub>2</sub> + ethane, which were optimized individually. The numerical values for the coefficients in eq 11 are given in Table 6 for each type of interaction parameter.

#### 4. RESULTS AND DISCUSSION

In the following sections we analyze the performance of the obtained correlation of parameters, both for representing the phase behavior of CO<sub>2</sub> + *n*-alkane systems considered in the optimization and for predicting the phase behavior for those CO<sub>2</sub> + *n*-alkane systems not included in the objective function. The prediction of densities for different types of equilibrium and systems is also analyzed. For most of the figures prepared, we selected systems and conditions for which experimental data sets from different laboratories were available and could be compared. The results for a few CO<sub>2</sub> + *n*-alkane systems adjusted individually, including the CO<sub>2</sub> + methane and CO<sub>2</sub> + ethane cases, will also be presented and discussed as an alternative when the correlation predictions are not accurate enough.

**4.1. Evolution of Phase Behavior Along the CO<sub>2</sub> + *n*-Alkane Homologue Series, as Predicted from the Correlation.** The type of phase behavior predicted for CO<sub>2</sub> + *n*-tridecane is, naturally, quite sensitive to interaction parameters, whatever equation of state and mixing rules used, and frequently, either type II or type III is predicted for this system (see refs 16 and 17). During our optimization process, we found that something similar applies to the CO<sub>2</sub> + methane system, since, surprisingly, the phase behavior for this system (sometimes assumed as a typical case of type I) is not far from being of type III. Nevertheless, the correlation summarized in eq 11 and Table 6 [complemented with parameters for the first two (CO<sub>2</sub> + C1 and CO<sub>2</sub> + C2) systems in Table B4 in the Supporting Information] correctly predicts the type of fluid phase behavior for all the binary systems in the CO<sub>2</sub> + *n*-alkane series, that is, type II up to C12, type IV for C13, and type III from C14 on. This can be seen in Figure 3 which shows the evolution of the CO<sub>2</sub> + *n*-alkane phase behavior with the

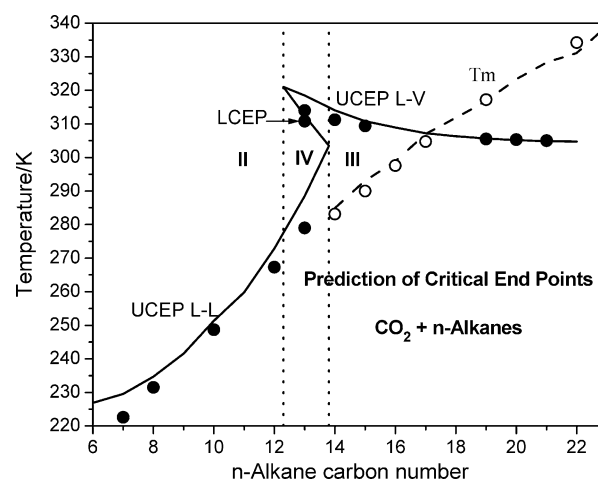
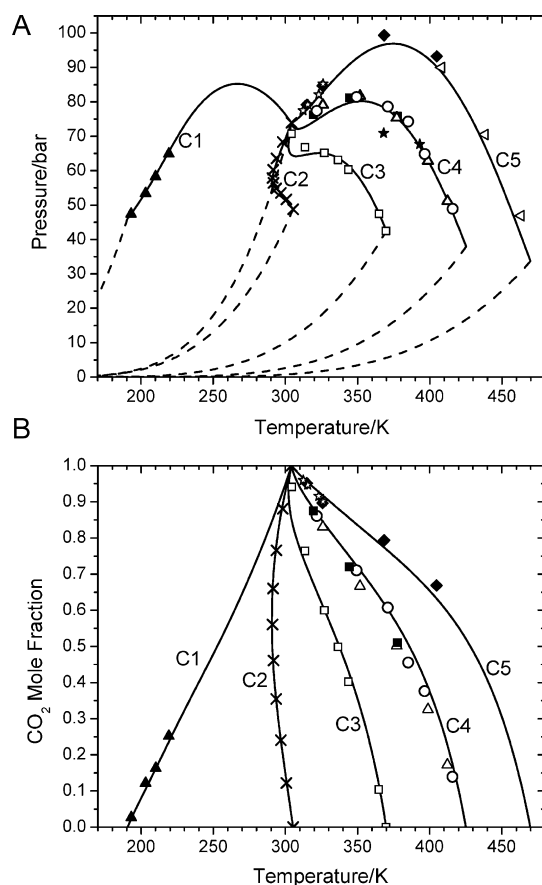


Figure 3. Experimental critical end points (CEPs, Table A1 in the Supporting Information, full circles) and CEPs predicted from the parameters correlation in eq 11 and Table 6 (solid line) for the CO<sub>2</sub> + *n*-alkane homologue series. The boundaries (vertical dotted lines) between types II–IV and IV–III are approximately sketched in the figure, only for illustrative purposes. Predicted  $T_m$  values are also shown (dashed line) and compared to experimental values (empty circles, Table 2 of ref 4). Model: RK-PR EOS with CMRs.

*n*-alkane CN, through calculated and experimental critical end point temperatures. Figure 3 also shows the experimental and predicted  $T_m$  values for type III systems, while Figures 4 and 5 present the evolution of liquid–vapor critical lines, both in the  $P$ – $T$  and  $x$ – $T$  spaces, for CO<sub>2</sub> + *n*-alkane systems containing from C1 to C5 and from C6 to C10, respectively. We remark that, within the CN range of Figures 4 and 5, only critical points for CO<sub>2</sub> + C1 and CO<sub>2</sub> + C2 (optimized individually) and for CO<sub>2</sub> + C3, CO<sub>2</sub> + C4, CO<sub>2</sub> + C6, CO<sub>2</sub> + C8, and CO<sub>2</sub> + C10 (part of the series optimization) were considered in the objective function (Table 2) through a single system-point by default and through two critical points for CO<sub>2</sub> + C1 and two critical points for CO<sub>2</sub> + C10 (Table 2). Still, the evolution of the calculated critical lines appears to be correct for all the systems from C1 to C10 when compared to experimental data. Moreover, although not shown in the figures, our parameters predict a virtual UCEP for CO<sub>2</sub> + C1 at 178.3 K, which is in agreement with the deep study on this system published by Rainwater.<sup>18</sup> Such UCEP is virtual because of the interference of solid–fluid transitions; that is, the UCEP is metastable. Rainwater<sup>18</sup> points out that “If the UCEP locus in Figure 3 of Miller and Luks<sup>19</sup> is extrapolated to a carbon number of one, a temperature of about 180 K is obtained”, and using a



**Figure 4.** Calculated critical lines for  $\text{CO}_2 + n$ -alkane binary systems from  $\text{CO}_2 + \text{methane}$  to  $\text{CO}_2 + n$ -pentane. From  $\text{CN} = 3$  to  $\text{CN} = 5$ , the calculations were performed using the parameters correlation in eq 11 and Table 6. For  $\text{CN} = 1$  and  $\text{CN} = 2$ , the interaction parameters were taken from Table B4 (Supporting Information). The dashed lines are calculated pure compound saturation curves. Markers: experimental critical points taken from references in Table A2 (Supporting Information). Model: RK-PR EOS with CMRs. Table B1 (Supporting Information) defines the labels of the  $n$ -alkanes.

nonclassical model, Rainwater<sup>18</sup> predicts an UCEP temperature of 181.9 K. This value is in good agreement with our value (i.e., 178.3 K) in spite of the fact that, opposite to Rainwater's model,<sup>18</sup> the present model does not explicitly account for nonclassical effects.

The evolution is also correct for the calculated critical lines shown in Figure 6 for carbon numbers from 13 to 22, considering the behavior of both the liquid–vapor and liquid–liquid parts of such critical lines, including the higher pressure region (the maximum pressure in Figure 6 is 1000 bar). Note that no ad hoc weight factors have been used in this work in the objective function that eq 10 defines. Besides, only four experimental high-pressure critical points were considered for each one of four selected type III systems (see Table 3).

The compositions of the phases in liquid–liquid–vapor equilibrium are presented in Figure 7 for the  $\text{CO}_2 + n$ -alkane systems. The experimental data (markers) correspond only to the liquid phases at LLVE. The predictions from eq 11 and Table 6 achieve a significantly better quantitative agreement with experimental data than that found in previous studies based on quadratic mixing rules, particularly for the alkane-rich phases (see refs 3 and 20). Note also the smooth and qualitatively correct evolution predicted when going from one

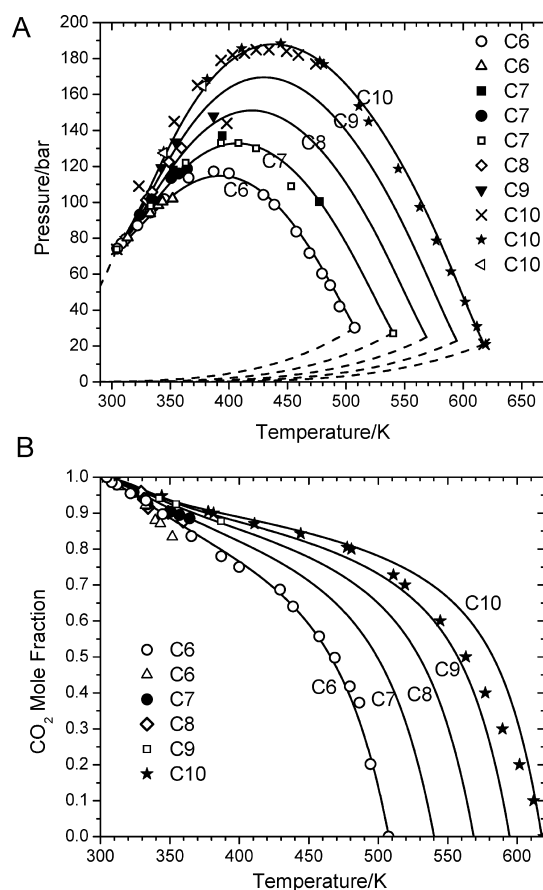


**Figure 5.** Critical lines for the binary systems of  $\text{CO}_2$  with  $n$ -hexane (C6) to  $n$ -decane (C10), calculated from the parameters correlation in eq 11 and Table 6. Dashed lines are calculated pure compound saturation curves. Markers: experimental critical points taken from references in Table A2 (Supporting Information). Model: RK-PR EOS with CMRs. Table B1 (Supporting Information) defines the labels of the  $n$ -alkanes.

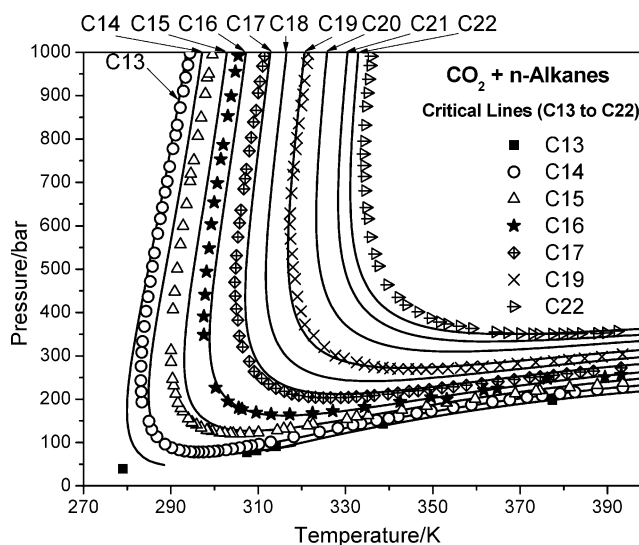


**Figure 6.** Critical lines for the binary systems of  $\text{CO}_2$  with  $n$ -tridecane (C13) to  $n$ -docosane (C22), calculated from the parameter correlation in eq 11 and Table 6. Markers: experimental critical points taken from references in Table A2 (Supporting Information). Model: RK-PR EOS with CMRs. Table B1 (Supporting Information) defines the labels of the  $n$ -alkanes.

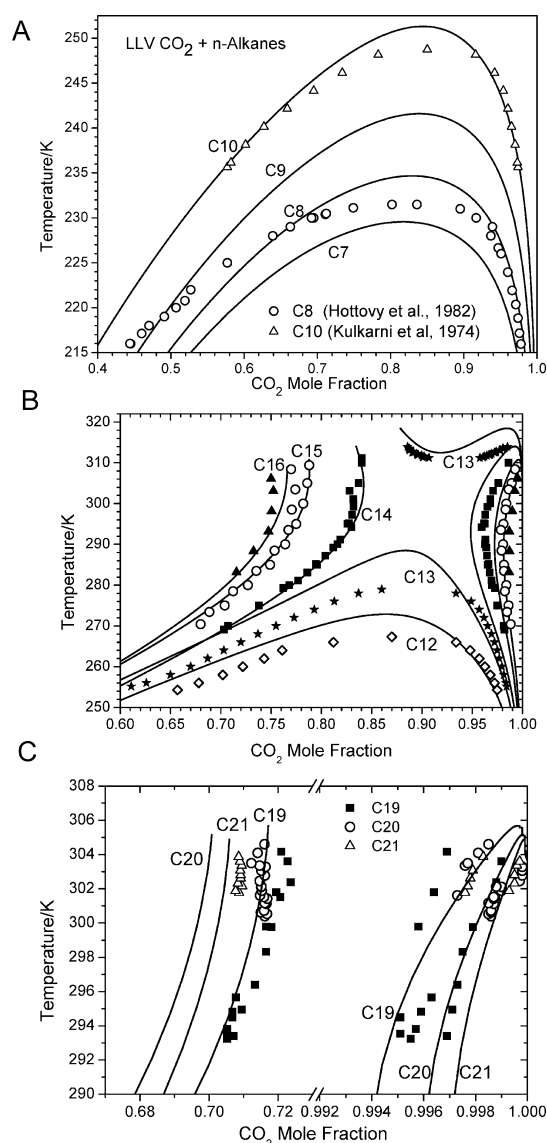


**Figure 7.** Liquid-liquid-vapor (LLV) equilibrium in the temperature-composition space, for  $\text{CO}_2$  +  $n$ -alkane binary systems from  $\text{CO}_2$  + C7 to  $\text{CO}_2$  + C21. Markers: Experimental data taken from Hottovy et al. 1982 (C8), Kulkarni et al. (C10), van der Steen et al. (C14–C15–C16), Fall and Luks (C13), Hottovy et al. 1981 (C12–C13–C14–C15, ) and Fall et al., (C19–C20–C21). Lines were calculated from the parameter correlations in eq 11 and Table 6. Model: RK-PR EOS with CMRs. Table B1 (Supporting Information) defines the labels of the  $n$ -alkanes.

binary system to the next one, and that only one intersection point is observed. This, which is quite likely to be an artificial outcome of the model, happens between the C13 and C14 curves in the low temperature region for lines describing the composition of the alkane-rich liquid phase at LLVE. This type of experimentally not confirmed intersection points is usually more frequent when using QMRs (these intersections were explicitly shown by Cismondi<sup>20</sup> and seem to occur also in results by Polishuk et al.<sup>3</sup>). We also found multiple intersection points in our early attempts to correlate the phase equilibria of the  $\text{CO}_2$  +  $n$ -alkane homologue series with CMRs.

The only qualitatively surprising effect found in the predictions, which is opposed to the behavior of the experimental data, is the position of the heavy liquid branch for the system

$\text{CO}_2$  + C20 (Figure 7), showing the lowest (instead of intermediate)  $\text{CO}_2$  content, with respect to those for the systems  $\text{CO}_2$  + C19 and  $\text{CO}_2$  + C21. As discussed in the next section, this result could be related to the inclusion of two “bad” data points for the system with  $n$ -eicosane (C20). The unwanted behavior found for the predicted  $\text{CO}_2$  content of the  $n$ -alkane rich liquid phase at LLV equilibrium, could have been avoided by introducing proper inequality restrictions when optimizing the description of the phase equilibria of the  $\text{CO}_2$  +  $n$ -alkane series.

At a quantitative level, it can be observed from Figure 7 that there would still be room for further improvement of the LLV description for some systems, specially for the  $\text{CO}_2$  + C8 and  $\text{CO}_2$  + C13 mixtures. Figure 8 shows the predictions from

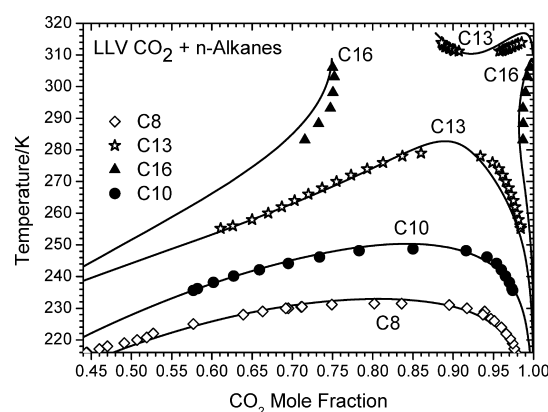


**Figure 8.** Liquid-liquid-vapor (LLV) equilibrium in the temperature-composition space, for some  $\text{CO}_2$  +  $n$ -alkane binary systems, predicted from parameters in Table B4 (Supporting Information). Markers: Experimental data points taken from the same references indicated for Figure 7. Model: RK-PR EOS with CMRs. Table B1 (Supporting Information) defines the labels of the  $n$ -alkanes.

the individually obtained sets of parameters in Table B4 (Supporting Information), for the systems  $\text{CO}_2$  + C8,  $\text{CO}_2$  + C10,  $\text{CO}_2$  + C13, and  $\text{CO}_2$  + C16. We must remark that these parameters are not the result of correlating a large number of “binary system-specific” experimental data of only a LLV nature but rather the result of minimizing the objective function for each binary system, considering all corresponding experimental data in Tables 2–5, and Tables B2 and B3 in the Supporting Information, where the critical end point temperatures and liquid compositions at LLV equilibrium for only one temperature per system are complemented with other type of data for different conditions. To fix ideas, the curve labeled “C8” in Figure 8 is a prediction from binary parameters specific of the  $\text{CO}_2$  + C8 system (Table B4, Supporting Information) that were fitted from the following experimental information of the  $\text{CO}_2$  + C8 system: one critical point (Table 2), the UCEP temperature (Table 4), and one LLV point (Table 5).

**4.2. Description of Two-Phase Equilibria for Systems Considered in the Optimization.** Figures 9–15 show different Pxy diagrams for the binary mixtures of  $\text{CO}_2$  with methane, ethane, propane,  $n$ -butane,  $n$ -hexane,  $n$ -decane, and  $n$ -hexadecane, all of them having contributed with data considered in the objective functions (Tables 2–5 and Tables B2 and B3 in the Supporting Information). The description of vapor-liquid equilibria appears to be very accurate in comparison to experimental data for the systems of  $\text{CO}_2$  with methane (Figure 9) and ethane (Figure 10), which were optimized (each of them individually, Table B4, Supporting

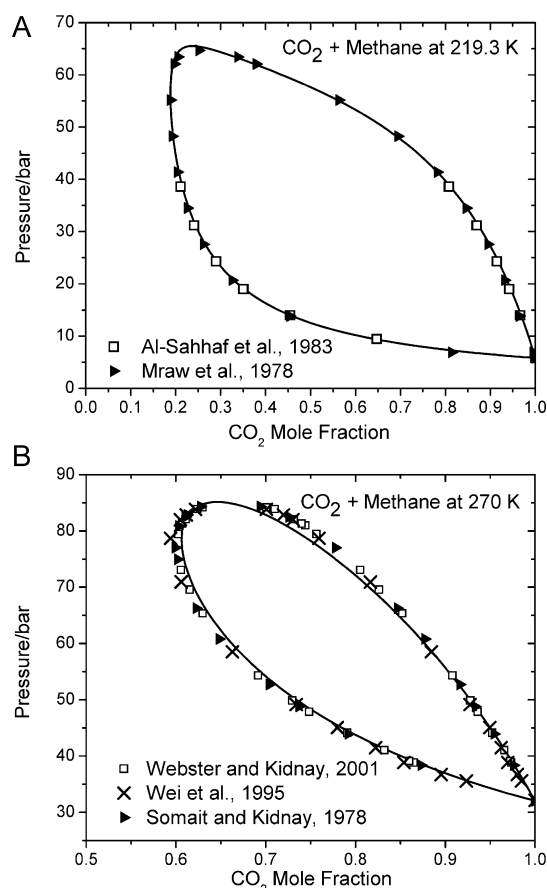


**Figure 9.** Isothermal two-phase equilibrium (Pxy) diagrams for  $\text{CO}_2$  + methane (C1), calculated from parameters in Table B4 in the Supporting Information (solid lines). Markers: experimental data taken from references in Table A4 (Supporting Information). Model: RK-PR EOS with CMRs.

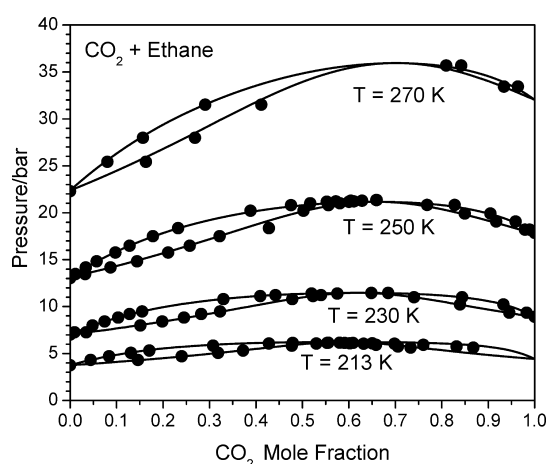


**Figure 10.** Predicted isothermal two-phase equilibrium (Pxy) diagrams for  $\text{CO}_2$  + ethane (C2), calculated from parameters in Table B4, Supporting Information, (solid lines). Markers: Experimental points taken from references in Table A4 (Supporting Information). Model: RK-PR EOS with CMRs.

Information) separately from the rest of the series. Predictions for the other systems (Figures 11–15) are also quite successful, with some exceptions regarding bubble pressures. In particular, a systematic shift of the liquid branches to higher  $\text{CO}_2$  mole

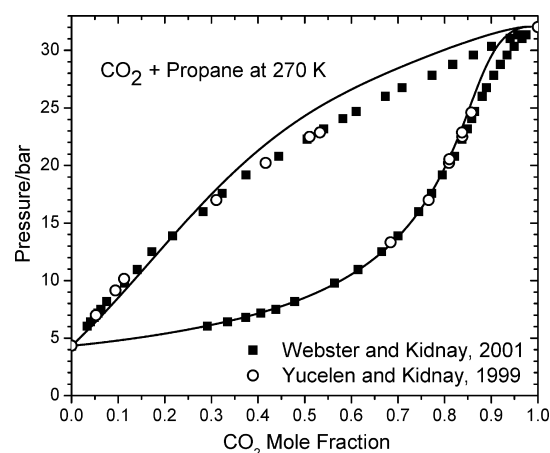


**Figure 11.** Isothermal two-phase equilibrium (Pxy) diagram for  $\text{CO}_2$  + propane (C3) at 270 K, calculated (solid lines) from the parameter correlation in eq 11 and Table 6. Markers: experimental data taken from references in Table A4 (Supporting Information). Model: RK-PR EOS with CMRs.

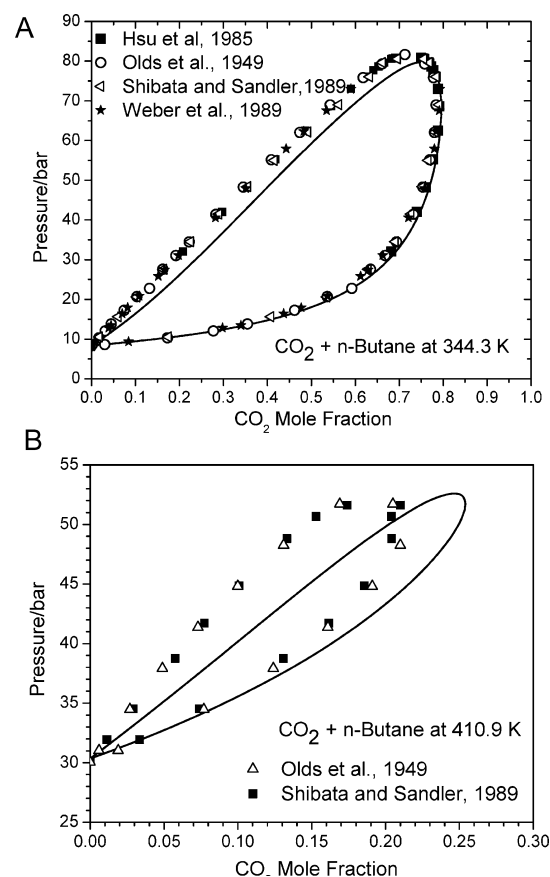


**Figure 12.** Isothermal two-phase equilibrium (Pxy) diagrams for  $\text{CO}_2$  + *n*-butane (C4), calculated (solid lines) from the parameter correlation in eq 11 and Table 6. Markers: experimental data taken from references in Table A4 (Supporting Information). Model: RK-PR EOS with CMRs.

fractions is observed for the mixtures  $\text{CO}_2$  + C4 (Figure 12) and  $\text{CO}_2$  + C6 (Figure 13) and, to a lesser extent, also for the system  $\text{CO}_2$  + C10 (Figure 14). This effect is more evident in the diagram with *n*-butane at 410.9 K (Figure 12). It is important to note that, in predictions or correlations from



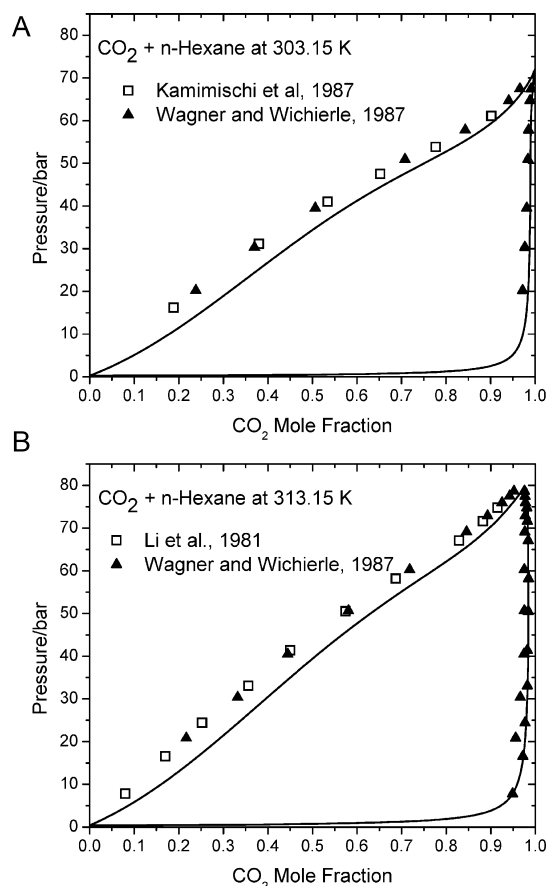


**Figure 13.** Isothermal two-phase equilibrium (Pxy) diagrams for  $\text{CO}_2$  + *n*-hexane (C6), calculated (solid lines) from the parameter correlation in eq 11 and Table 6. Markers: experimental data taken from references in Table A4 (Supporting Information). Model: RK-PR EOS with CMRs.

other authors,<sup>17,21,22</sup> relatively larger errors are also found at high temperatures close to the *n*-butane critical point, when comparing to lower temperatures for  $\text{CO}_2$  + *n*-butane. Notice in Figure 12 that the size of the vapor–liquid equilibrium region is much smaller at 410.9 K than at 344.3 K.

In view of the excellent results when correlating individual systems, which were illustrated in Figures 8–10, the deviations observed for liquid phases in Figures 11–14 could be possibly ascribed to a deficiency of the specific polynomial series correlation (eq 11 and Table 6) in the CN range from 3 to 10 rather than to the CMRs.

Note that the results, for example in Figure 9 for  $\text{CO}_2$  + methane, show the same or higher level of accuracy, than correlations using a more theoretical and complex model like PCP-SAFT (Figure 15 in Tang et al.<sup>23</sup>).

Figure 16 shows the Pxy diagram for  $\text{CO}_2$  + *n*-hexadecane at 333.2 K, for which three sets of experimental data from different authors are available. Note that no experimental data points at this temperature were considered in the objective function for obtaining the constants of Table 6 for the  $\text{CO}_2$  + *n*-alkane homologue series correlation. Then, the predictions shown in Figure 16 can be regarded as an interpolation between data for  $\text{CO}_2$  + *n*-hexadecane (and other systems) at different temperatures. The data from D'Souza et al.<sup>24</sup> and Holscher et al.<sup>25</sup> agree quite well among themselves and also with the predictions. Instead, the data from Charoensombut-Amon et al.,<sup>11</sup> are shifted to higher  $\text{CO}_2$  molar fractions, specially in the critical region. In

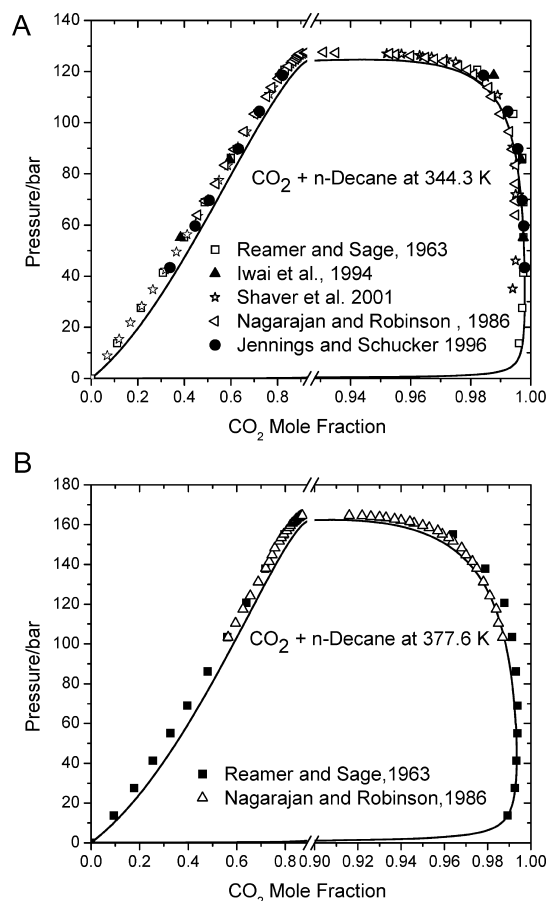


**Figure 14.** Isothermal two-phase equilibrium (Pxy) diagrams for  $\text{CO}_2$  + *n*-decane (C10), calculated (solid lines) from the parameter correlation in eq 11 and Table 6. Markers: experimental data taken from references in Table A4 (Supporting Information). Model: RK-PR EOS with CMRs.

spite of such shift, this time the observed critical pressure (but not the critical composition) reasonably agrees with other experimental studies (this was not the case at 313.2 K in Figure 1).

Predictions for  $\text{CO}_2$  + *n*-eicosane are in excellent agreement with data from Huie et al.<sup>26</sup> and from Sato et al.<sup>27</sup> as shown in Figure 17. At the same time, the figure suggests that data reported by Kordikowski and Schneider<sup>28</sup> for 353.2 and 393.2 K might suffer from a systematic underestimation of  $\text{CO}_2$  content in the liquid phase. It is remarkable that, even when the equilibrium points for both temperatures at 250 bar were taken from this source (Kordikowski and Schneider<sup>28</sup>) and included in the objective function (Table B2, Supporting Information), the optimization results lead to predictions at 353.2 and 393.2 K that reasonably agree in the light phase but clearly disagree with those data points at 250 bar in the liquid phase [note, the high values of OF and  $\text{OF}_{\text{corr}}$  for  $\text{CO}_2$  + C20 in the last column of Table B4 (Supporting Information), even when other systems have contributed more terms to the series objective function]. Instead, predictions reproduce well other data for  $\text{CO}_2$  + C20 and neighbor  $\text{CO}_2$  + *n*-alkane systems, which show a smooth and coherent evolution of the series. Still, these conflictive points at 250 bar may have influenced the results to some extent, bringing the liquid branches to lower  $\text{CO}_2$  content, and this could be related to the unexpected position of the predicted heavy liquid phase branch for  $\text{CO}_2$  + C20 in Figure 7, previously pointed out. It is usually difficult to establish whether different experimental data sets for different

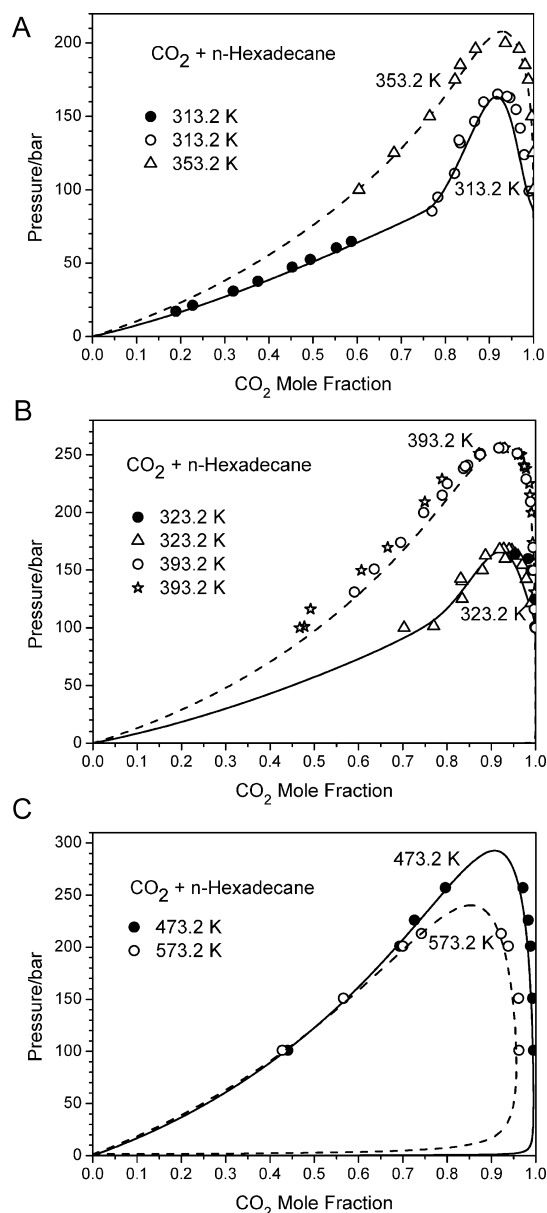


**Figure 15.** Isothermal two-phase equilibrium (Pxy) diagrams for  $\text{CO}_2$  + *n*-hexadecane (C16), calculated (lines) from the parameter correlation in eq 11 and Table 6. Markers: experimental data taken from references in Table A4 (Supporting Information): Tanaka et al. (313.2 K), Nieuwoudt and du Rand (313.2 and 323.2 K), Pöhler (323.2 K), Kordikowski and Schneider (353.2 K), Spee and Schneider (393.2 K), Holscher et al. (393.2 K) and Brunner et al. (473.2 and 573.2 K). Only points for two pressures at 393.2 K and two pressures at 573.2 K were considered in the correlation (Table B2, Supporting Information). Model: RK-PR EOS with CMRs.

conditions, or even for different binary systems in the same homologue series, are in agreement, that is, whether they are consistent with a reasonable evolution of the phase behavior in the series. The case of Figure 17 illustrates how a good correlation of the series, at least within a certain carbon number range, can help; that is, this is a case where a correlation of phase equilibria of a homologue series as a whole can be used to identify sets of experimental data which may have a high level of error. More specifically, Figure 17 and the accompanying analysis suggest that the phase equilibrium data for  $\text{CO}_2$  + C20 by Kordikowski and Schneider<sup>28</sup> are, to some

extent, inaccurate. This should be taken as a provisional conclusion that should be confirmed or rejected through carefully carried out new experiments, at the conditions of Figure 17, if possible, by different laboratories.

We want to point out that the correct prediction of bubble pressures in the low  $\text{CO}_2$  content region for the systems  $\text{CO}_2$  + C16 and  $\text{CO}_2$  + C20 (Figures 15–17) was not such in our first

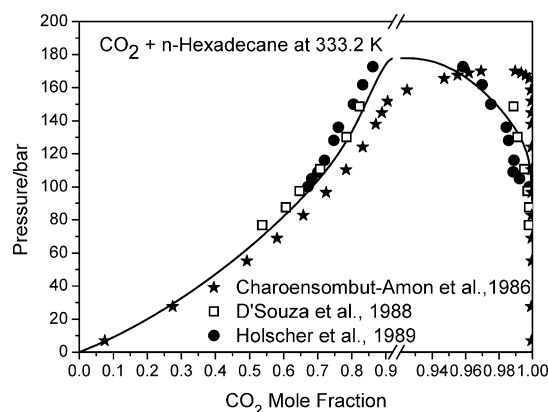


**Figure 16.** Isothermal two-phase equilibrium (Pxy) diagram for  $\text{CO}_2$  + *n*-hexadecane (C16) at 333.2 K, calculated (solid lines) from the parameter correlation in eq 11 and Table 6, and comparison to three different sets of experimental data (markers) in mutual disagreement. References included in Table A4 (Supporting Information). Model: RK-PR EOS with CMRs.

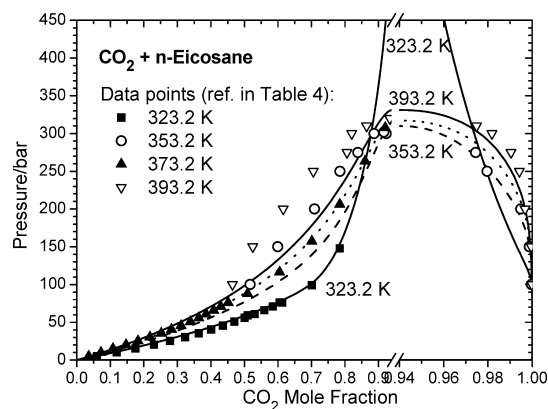


**Figure 17.** Isothermal two-phase equilibrium (Pxy) diagrams for  $\text{CO}_2$  + *n*-eicosane (C20), calculated (lines) from the parameter correlation in eq 11 and Table 6. Markers: experimental data taken from references in Table A4 (Supporting Information). Within the temperature range of the present figure only points for 250 bar at 353.2 and 393.2 K (Table B2, Supporting Information) and one bubble pressure at 373.2 K (Table B3, Supporting Information) were considered in the correlation. Model: RK-PR EOS with CMRs.

attempts to correlate the  $\text{CO}_2$  + *n*-alkane series. That was surprising at first, since experience with QMRs told us that this should be an easy test, and usually only the critical or high pressure region is difficult to predict or even correlate. However, the flexibility of CMRs and the bifurcation that takes place for example for a symmetric QMRs  $k_{12}$  interaction parameter into the CMRs  $k_{112}$  and  $k_{122}$  parameters, that govern the two binary infinite dilution ends, led us to identify the need of introducing bubble pressure experimental data of lower pressure in the objective function (see data at around 20 bar in Table B3 in the Supporting Information).

Figures 18–20 present the isothermal Pxy diagrams for the mixtures of different heavy *n*-alkanes with CO<sub>2</sub> at 373.2, 393.2,

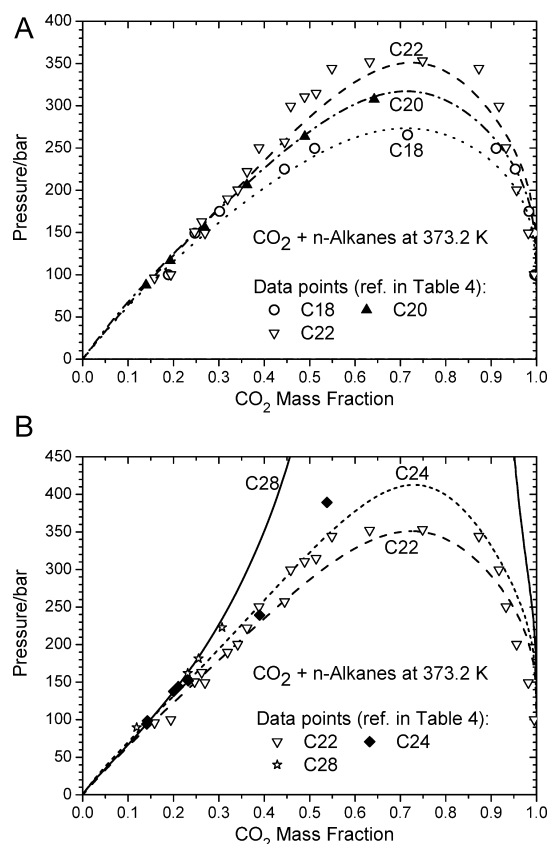


**Figure 18.** Isothermal two-phase equilibrium (Pxy) diagrams for binary mixtures of CO<sub>2</sub> with different heavy *n*-alkanes at 373.2 K, calculated (lines) from the parameter correlation in eq 11 and Table 6. Markers: experimental data taken from references in Table A4 (Supporting Information). Model: RK-PR EOS with CMRs. Table B1 (Supporting Information) defines the labels of the *n*-alkanes.

and 423.2 K, respectively. Notice that, in all three figures, we have plotted the pressure as a function of the CO<sub>2</sub> mass fraction rather than as a function of the CO<sub>2</sub> mole fraction. This choice for the CO<sub>2</sub> concentration scale facilitates the interpretation of the figures. In general, and considering some level of uncertainty in the experimental data which is evident, the calculated curves agree well with the experimental points. A clear exception is the case of the system CO<sub>2</sub> + C32 (Figure 19 B) where we see a good agreement between the model and the experimental data only for the liquid phase below 310 bar. At 393.2 K, the system CO<sub>2</sub> + C32 presents, experimentally, a critical point with a critical pressure in the order of 640 bar (Figure 19 B), while the model (solid line) shows a higher degree of immiscibility. Evidently, the model predicts a *T<sub>m</sub>* value greater than the actual one. Notice that only three experimental points for the system CO<sub>2</sub> + C32, with a maximum pressure less than 51 bar, were used in CO<sub>2</sub> + *n*-alkane series objective function (Tables B2 and B3 in the Supporting Information).

The phase equilibrium experimental data for CO<sub>2</sub> + C20 at 373.2 K (Figure 18) and 423.2 K (Figure 20) are well reproduced by the model. This is not the case for CO<sub>2</sub> + C20 at 393.2 K in Figure 19, where the CO<sub>2</sub> + C20 experimental data,

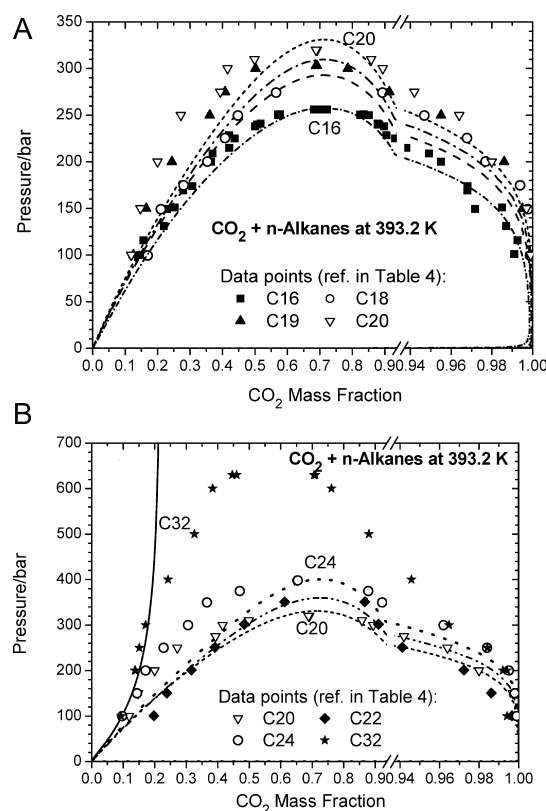


**Figure 19.** Isothermal two-phase equilibrium (Pxy) diagrams for binary mixtures of CO<sub>2</sub> with different heavy *n*-alkanes at 393.2 K, calculated (lines) from the parameter correlation in eq 11 and Table 6. Markers: experimental data taken from references in Table A4 (Supporting Information). Only two pressures for *n*-hexadecane at this temperature and one for *n*-eicosane were considered in the correlation (Table B2, Supporting Information). Model: RK-PR EOS with CMRs. Table B1 (Supporting Information) defines the labels of the *n*-alkanes.

previously detected as probably wrong, are from Kordikowski and Schneider.<sup>28</sup>

Again, a careful examination of the evolution of data sets in Figure 19 suggests that there would be important errors in the experimental liquid phase composition, for one or more data sets in Figure 19, since the data sets do not follow a clear trend with respect to the *n*-alkane CN.

**4.3. Prediction of Two-Phase Equilibria for Systems Not Considered in the Optimization.** This study is a first implementation of our approach for the parametrization of CMRs for a complete homologue series of binary systems. To analyze the possibilities and limitations of such an approach and to detect possible improvements, instead of intending to obtain the ultimate correlation for the CO<sub>2</sub> + *n*-alkane series, we deliberately left some CO<sub>2</sub> + *n*-alkane systems out of the objective function, even when there are important experimental phase equilibrium data available for them. The reason for that was to explore the predictive potential of the approach. Figures 21–23 show, respectively, the prediction of isothermal Pxy diagrams for the binary mixtures CO<sub>2</sub> + *n*-heptane (C7), CO<sub>2</sub> + *n*-dodecane (C12), and CO<sub>2</sub> + *n*-pentadecane (C15). For the system CO<sub>2</sub> + C7 (Figure 21) the deviations in the liquid phase are similar to those previously noticed for CO<sub>2</sub> + C4 (Figure 12), CO<sub>2</sub> + C6 (Figure 13), and CO<sub>2</sub> + C10 (Figure 14). Figures 22 and 23 show, in general, a good

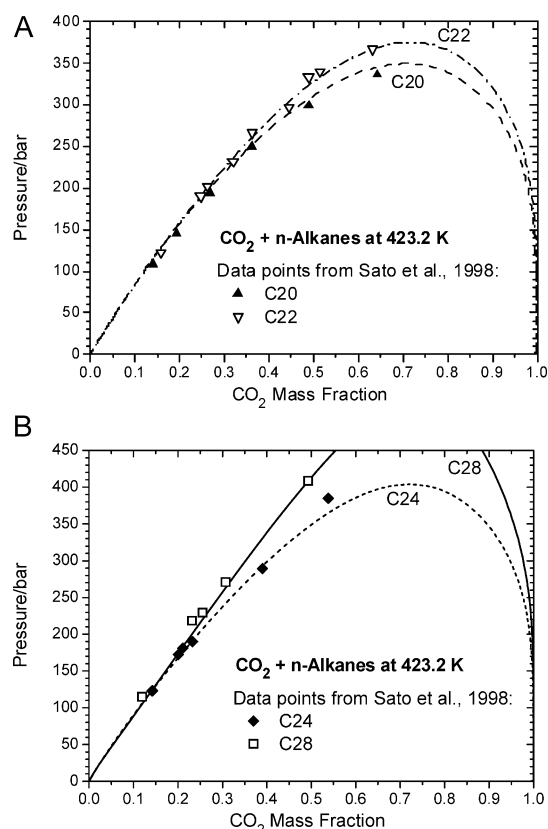


**Figure 20.** Isothermal two-phase equilibrium (Pxy) diagrams for binary mixtures of CO<sub>2</sub> with different heavy *n*-alkanes at 423.2 K, calculated (lines) from the parameter correlation in eq 11 and Table 6. Markers: experimental data taken from references in Table A4 (Supporting Information). Only one point at this temperature and for C28 (Table B3, Supporting Information) was considered in the correlation. Model: RK-PR EOS with CMRs. Table B1 (Supporting Information) defines the labels of the *n*-alkanes.

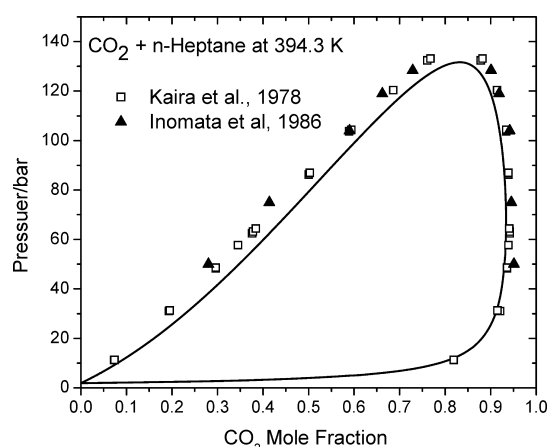


**Figure 21.** Predicted isothermal two-phase equilibrium (Pxy) diagram for CO<sub>2</sub> + *n*-heptane (C7), calculated (solid lines) from the parameter correlation in eq 11 and Table 6. Markers: experimental data taken from references in Table A4 (Supporting Information). Model: RK-PR EOS with CMRs. No experimental data for the system CO<sub>2</sub> + *n*-heptane were used in the objective function whose minimization led to the parameter values of Table 6.

agreement with experimental data, considering that they correspond to pure predictions.

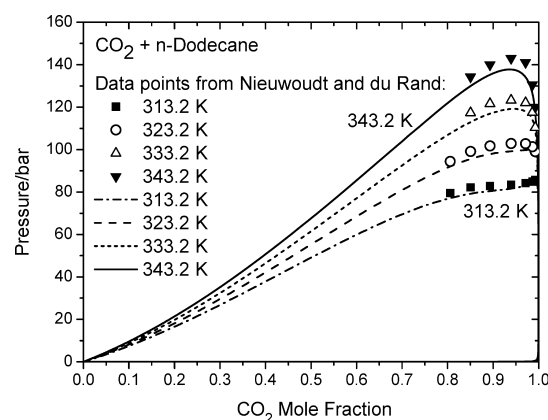


**Figure 22.** Predicted isothermal two-phase equilibrium (Pxy) diagrams for CO<sub>2</sub> + *n*-dodecane (C12), calculated (lines) from the parameter correlation in eq 11 and Table 6. Markers: experimental data taken from references in Table A4 (Supporting Information). Model: RK-PR EOS with CMRs. No experimental data for the system CO<sub>2</sub> + *n*-dodecane were used in the objective function whose minimization led to the parameter values of Table 6.

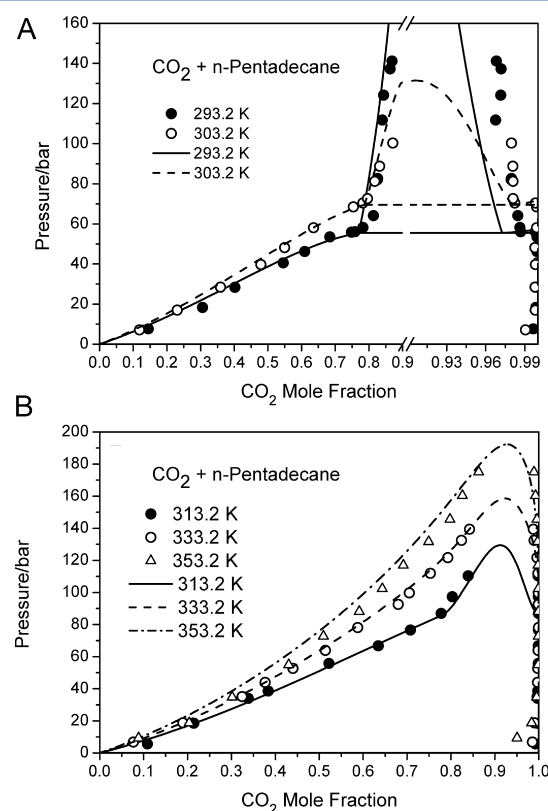


**Figure 23.** Predicted isothermal two-phase equilibrium (Pxy) diagrams for CO<sub>2</sub> + *n*-pentadecane (C15), calculated (lines) from the parameter correlation in eq 11 and Table 6. Markers: experimental data taken from references in Table A4 (available in the Supporting Information). Model: RK-PR EOS with CMRs. No experimental data for the system CO<sub>2</sub> + *n*-pentadecane, were used in the objective function whose minimization led to the parameter values of Table 6.

**4.4. Prediction of Densities.** As it can be concluded from Tables A2–A6 (in the Supporting Information), there is a limited amount of published density data available, in comparison to compositional data, for the series of CO<sub>2</sub> + *n*-alkane binary mixtures. Still, there are some sets of density data



reported for different types of equilibrium, which are important for testing the predictions of density when correlating phase equilibrium in the  $P$ - $T$ - $x$  space. Figure 24 shows good

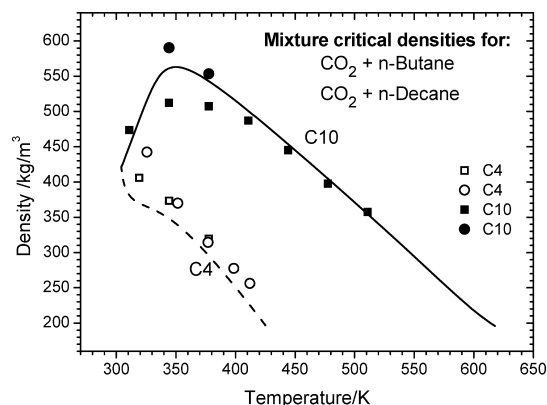


**Figure 24.** Critical lines, in the density–temperature space, for the binary systems of  $\text{CO}_2$  with  $n$ -butane (C4) and  $n$ -decane (C10). Lines predicted from the parameter correlation in eq 11 and Table 6. Markers: Experimental critical points taken from references in Table A2 (Supporting Information). No binary experimental density data were used while fitting the parameters reported in Table 6. Model: RK-PR EOS with CMRs.

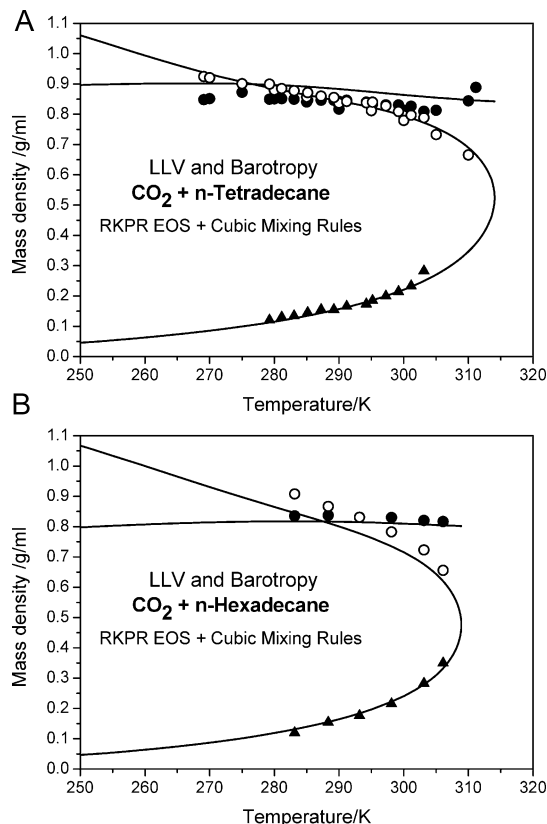


**Figure 25.** Prediction of density and barotropy along the liquid–liquid–vapor (LLV) equilibrium region, for the binary systems of  $\text{CO}_2$  with  $n$ -tetradecane (C14) and  $n$ -hexadecane (C16). Lines predicted from the parameters correlation in eq 11 and Table 6. Markers: Experimental densities at LLV equilibrium taken from references in Table A3 (Supporting Information). No binary experimental density data were used while fitting the parameters reported in Table 6. Model: RK-PR EOS with CMRs.

agreement in the critical lines for  $\text{CO}_2$  + C4 and  $\text{CO}_2$  + C10. This applies also to the barotropy phenomenon along the LLV line, as can be seen in Figure 25 for  $\text{CO}_2$  + C14 and  $\text{CO}_2$  + C16. The error in the predicted barotropic temperatures is around 10 and 5 K, respectively. A comparison to Figure 12 of our previous work<sup>1</sup> confirms that it was appropriate to change the pure compound RK-PR parameters, as already discussed in section 3.1, where the pure compound volumetric information used to obtain the pure compound RK-PR parameters is indicated.

Figures 26 and 27 show isothermal liquid–vapor equilibrium density curves for the systems  $\text{CO}_2$  + C4 and  $\text{CO}_2$  + C10

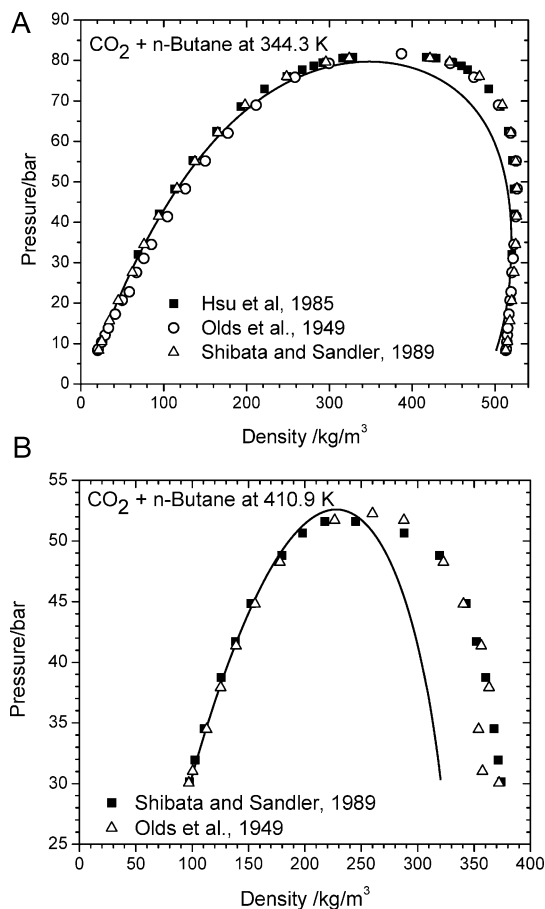


**Figure 26.** Isothermal two-phase equilibrium pressure–density diagrams for  $\text{CO}_2$  +  $n$ -butane (C4), calculated (solid lines) from the parameter correlation in eq 11 and Table 6. Markers: experimental data taken from references in Table A4 (available in the Supporting Information). No binary experimental density data were used while fitting the parameters reported in Table 6. Model: RK-PR EOS with CMRs. The corresponding Pxy diagrams are shown in Figure 12.

at the same temperatures considered in Figures 12 and 14. The only important discrepancy observed between data and predictions, that is, the underestimation of saturated liquid densities by 10–15% in Figure 26 at 410.9 K, is clearly related both to the corresponding liquid branch composition shift in Figure 12, previously pointed out, and to the underestimation of saturated liquid densities for pure compounds ( $n$ -butane in this case) as the critical pure compound temperature is approached. On the other hand, the degree of

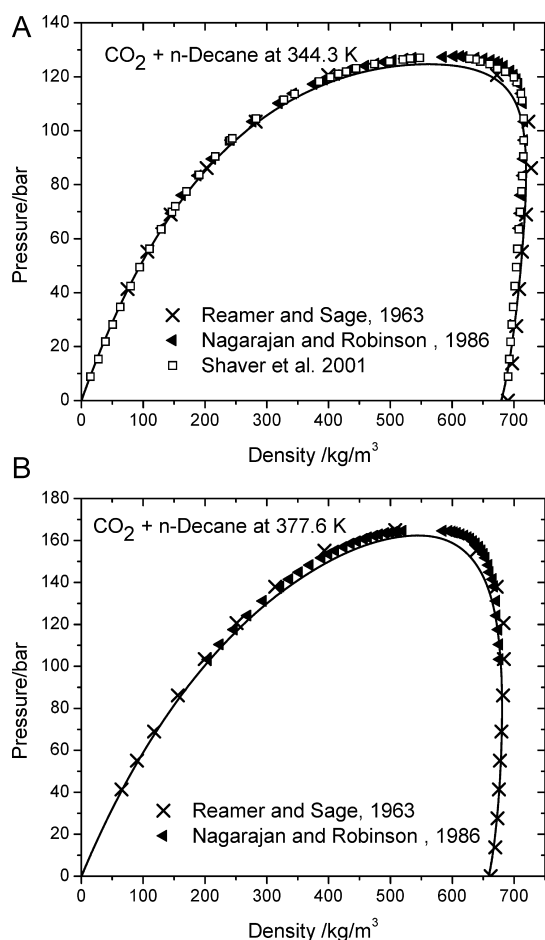


**Figure 27.** Isothermal two-phase equilibrium pressure–density diagrams for  $\text{CO}_2 + n$ -decane (C10), calculated (solid lines) from the parameter correlation in eq 11 and Table 6. Markers: experimental data taken from references in Table A4 (available in the Supporting Information). No binary experimental density data were used while fitting the parameters reported in Table 6. Model: RK-PR EOS with CMRs. The corresponding Pxy diagrams are shown in Figure 14.

agreement between experimental and predicted densities is remarkably good for  $\text{CO}_2 + \text{C}_{10}$  in Figure 27.

**4.5. Final Remarks.** The description of the fluid phase equilibria of the  $\text{CO}_2 + n$ -alkane homologue series, obtained from the (series-specific) correlation defined by eq 11 and Table 6, and illustrated in the previous sections, for vapor–liquid and liquid–liquid regions and for the supercritical region of  $\text{CO}_2$ , is, to our knowledge, the most accurate series-specific description presented so far in the literature for  $\text{CO}_2 + n$ -alkane binary systems, at least for  $n$ -alkane carbon numbers from 10 on.

Although the eq 11/Table 6 correlation could be recommended for predicting  $\text{CO}_2 + n$ -alkane binary phase equilibria, particularly in the CN range from intermediate molecular weight to heavier  $n$ -alkanes, we need to remark that it was not our intention to develop, at this stage, something such as the best possible series-specific correlation using CMRs.

The goal of further improving such correlation, with a model like the one used here (RK-PR + CMRs), which offers high flexibility but simultaneously sets an important challenge for its parametrization, requires the availability of a first study for the whole  $\text{CO}_2 + n$ -alkane series, such as the present one. The development of this work led us to become aware of the relative importance and limitations of different aspects related

to the process of building a series-specific correlation. For instance, important issues related to the objective function are the definition of the terms, which was improved with respect to our previous work, the balance between different types of experimental data and the effect of not including certain experimental points.

Especially, the systematic deviations observed for carbon numbers up to 10 in the alkane-rich liquid composition (Figures 11 to 14) could be partially attributed to some limitations of the polynomial form. This functional form does not set reasonable limits for CN tending either to zero or to infinity. Besides, it would be interesting to explore in the future the use of the interval-Newton approach (INA) for minimizing the objective function of the series. According to Gau and Stadtherr,<sup>29</sup> the INA is a general-purpose technique, applicable to parameter estimation problems of considerable size, that offers mathematical and computational guarantees that the global optimum has been found. This is, however, achieved at the expense of higher computation times in comparison to local methods, which do not provide the mentioned guarantees. Exploring the use of the INA could be carried out through a constrained formulation or through an unconstrained formulation established by incorporating the model equations into the objective function.

It is therefore clear that there would be room for improving the predictive correlation obtained here for describing the phase equilibria of the  $\text{CO}_2 + n$ -alkane homologue series of binary systems.

In other words, and in view of the complexity of the problem of parametrizing a complete series, that is, of the diversity of aspects affecting the objective function and of the high flexibility of CMRs which can be hard to manage, we consider that it is important to report suboptimal results like the ones presented here, discussing limitations of procedures or approaches that we have already overcome and also the problems that still need to be fixed or the aspects that would require further study and improvement.

## 5. CONCLUSIONS

As a part of the required work for developing a predictive correlation for the fluid phase equilibria of the  $\text{CO}_2 + n$ -alkane homologue series, nearly 100 references containing phase equilibrium data for the series of  $\text{CO}_2 + n$ -alkane binary systems have been identified and classified in six tables. A strategy for the development of a correlation of cubic mixing rules (CMRs) interaction parameters for the whole series of  $\text{CO}_2 + n$ -alkane binary systems was discussed and implemented. A correlation, defined by a set of fourth order polynomials, valid for the binary systems from  $\text{CO}_2 + \text{C}_3$  to  $\text{CO}_2 + \text{C}_{32}$ , was obtained from the minimization of an objective function (OF). This OF considered a relatively small number of selected experimental fluid phase equilibrium data points of some  $\text{CO}_2 + n$ -alkane binary systems. The correlative and predictive capacities of the correlation are very good in general for the different types of fluid phase equilibria. However, some limitations were observed in the description of the liquid phase composition for carbon numbers up to C10, that is, an overestimation of the  $\text{CO}_2$  content of such phase.

A variety of recommendations have been provided, in order to get a good description of the phase behavior from flexible models like CMRs, based on our experience and on the issues we identified when designing an objective function for a series

with a complex phase behavior such as the CO<sub>2</sub> + *n*-alkane series.

The correlation of specific experimental data or the optimization of a single binary CO<sub>2</sub> + *n*-alkane system can be preferable when accuracy is required for particular applications and good and enough data are available. It has been shown that, when that is not the case, the correlation of a series of binary systems as a continuum entity can compensate for the partial lack of experimental data for some systems and even provide good predictions for those systems with no data available at all. The flexibility of CMRs allowed us to obtain a good description of the complex phase behavior of the series of asymmetric CO<sub>2</sub> + *n*-alkane binary systems. The availability of this type of predictive correlation can also be important in applications like CO<sub>2</sub>-enhanced oil recovery (EOR), where a mixture of an important number of compounds of the same family, differing in molecular weight, are put in contact with one solvent.

Although we have focused in this work on the phase behavior of the highly non ideal CO<sub>2</sub> + *n*-alkane series, the CMRs and the methodology here proposed for generating a series-specific correlation could be applied to other series with a complex phase behavior. Examples of them are the water + hydrocarbon series or the series of binary systems made of a light solvent, for example, CO<sub>2</sub>, ethane, or propane and an alkyl-ester, a primary alcohol, or a long tailed organic acid. For binary systems with association effects, for example, with hydrogen bonding, we expect the CMRs interaction parameters to account for them, even when such effects are not explicitly considered by the CMRs.

The present approach could be used to identify existing experimental binary phase equilibrium data sets potentially having high systematic errors. It would also be applicable to the identification of convenient conditions to carry out phase equilibrium measurements for binary systems with no experimental information available in the literature.

## ■ ASSOCIATED CONTENT

### ■ Supporting Information

Appendix A: literature review. Appendix B: additional tables. This information is available free of charge via the Internet at <http://pubs.acs.org/>.

## ■ AUTHOR INFORMATION

### Corresponding Author

\*E-mail: [mzabaloy@plapiqui.edu.ar](mailto:mzabaloy@plapiqui.edu.ar); [mcismondi@efn.uncor.edu](mailto:mcismondi@efn.uncor.edu).

### Notes

The authors declare no competing financial interest.

## ■ ACKNOWLEDGMENTS

We acknowledge the financial support received from the following Argentinean institutions: Consejo Nacional de Investigaciones Científicas y Técnicas de la República Argentina, Agencia Nacional de Promoción Científica y Tecnológica de la República Argentina, Universidad Nacional del Sur, and Universidad Nacional de Córdoba.

## ■ REFERENCES

- (1) Cismondi, M.; Mollerup, J.; Brignole, E. A.; Zabaloy, M. S. Modeling the high-pressure phase equilibria of carbon dioxide-triglyceride systems: A parameterization strategy. *Fluid Phase Equilib.* **2009**, *281* (1), 40–48.
- (2) Hegel, P. E.; Mabe, G. D. B.; Pereda, S.; Zabaloy, M. S.; Brignole, E. A. Phase equilibria of near critical CO<sub>2</sub> + propane mixtures with fixed oils in the LV, LL, and LLV region. *J. Supercrit. Fluids* **2006**, *37* (3), 316–322.
- (3) Polishuk, I.; Wisniak, J.; Segura, H. Estimation of liquid–liquid–vapor equilibria using predictive EOS models. 1. Carbon dioxide–*n*-alkanes. *J. Phys. Chem. B* **2003**, *107* (8), 1864–1874.
- (4) Cismondi, M.; Mollerup, J. M.; Zabaloy, M. S. Equation of state modeling of the phase equilibria of asymmetric CO<sub>2</sub> + *n*-alkane binary systems using mixing rules cubic with respect to mole fraction. *J. Supercrit. Fluids* **2010**, *55* (2), 671–681.
- (5) Elliott, J. R.; Lira, C. T., *Introductory Chemical Engineering Thermodynamics*; Prentice-Hall PTR: Upper Saddle River, NJ, 1999.
- (6) Zabaloy, M. S. Cubic mixing rules. *Ind. Eng. Chem. Res.* **2008**, *47* (15), 5063–5079.
- (7) Cismondi, M.; Mollerup, J. Development and application of a three-parameter RK-PR equation of state. *Fluid Phase Equilib.* **2005**, *232* (1–2), 74–89.
- (8) van Konynenburg, P. H.; Scott, R. L. Critical lines and phase equilibria in binary van der Waals mixtures. *Philos. Trans. R. Soc., A* **1980**, *298* (495), 495–540.
- (9) Fall, D. J.; Luks, K. D. Liquid–liquid–vapor phase equilibria of the binary system carbon dioxide + *n*-tridecane. *J. Chem. Eng. Data* **1985**, *30* (3), 276–279.
- (10) Cismondi, M.; Michelsen, M. L. Global phase equilibrium calculations: Critical lines, critical end points, and liquid–liquid–vapor equilibrium in binary mixtures. *J. Supercrit. Fluids* **2007**, *39* (3), 287–295.
- (11) Charoensombut-Amon, T.; Martin, R. J.; Kobayashi, R. Application of a generalized multiproperty apparatus to measure phase equilibrium and vapor phase densities of supercritical carbon dioxide in *n*-hexadecane systems up to 26 MPa. *Fluid Phase Equilib.* **1986**, *31* (1), 89–104.
- (12) Polishuk, I. An empirical modification of classical mixing rule for the cohesive parameter: The triple interactions in binary systems considered. *Ind. Eng. Chem. Res.* **2010**, *49* (10), 4989–4994.
- (13) Fredenslund, A.; Mollerup, J. Measurement and prediction of equilibrium ratios for the C<sub>2</sub>H<sub>6</sub> + CO<sub>2</sub> system. *J. Chem. Soc., Faraday Trans. 1* **1974**, *70*, 1653–1660.
- (14) PRAXIS Scalar Function Optimization. [http://people.sc.fsu.edu/~jburkardt/f77\\_src/praxis/praxis.html](http://people.sc.fsu.edu/~jburkardt/f77_src/praxis/praxis.html) (Accessed October 14, 2010).
- (15) Brent, R. P. *Algorithms for Minimization without Derivatives*; Dover: Mineola, NY, 2002.
- (16) Polishuk, I.; Wisniak, J.; Segura, H. Simultaneous prediction of the critical and sub-critical phase behavior in mixtures using equations of state II. Carbon dioxide-heavy *n*-alkanes. *Chem. Eng. Sci.* **2003**, *58* (12), 2529–2550.
- (17) Vitu, S.; Privat, R.; Jaubert, J. N.; Mutelet, F. Predicting the phase equilibria of CO<sub>2</sub> + hydrocarbon systems with the PPR78 model (PR EOS and *kij* calculated through a group contribution method). *J. Supercrit. Fluids* **2008**, *45* (1), 1–26.
- (18) Rainwater, J. C. A nonclassical model of a type 2 mixture with vapor–liquid, liquid–liquid, and three-phase equilibria. *Int. J. Thermophys.* **2000**, *21* (3), 719–737.
- (19) Miller, M. M.; Luks, K. D. Observations on the multiphase equilibria behavior of CO<sub>2</sub>-rich and ethane-rich mixtures. *Fluid Phase Equilib.* **1989**, *44* (3), 295–304.
- (20) Cismondi, M. Ingeniería del equilibrio entre fases: Diagramas globales y modelado de mezclas asimétricas con CO<sub>2</sub>. PhD thesis, Universidad Nacional del Sur, Bahía Blanca, Argentina, 2006.
- (21) Fu, D.; Liang, L.; Li, X. S.; Yan, S.; Liao, T. Investigation of vapor–liquid equilibria for supercritical carbon dioxide and hydrocarbon mixtures by perturbed-chain statistical associating fluid theory. *Ind. Eng. Chem. Res.* **2006**, *45* (12), 4364–4370.
- (22) Thi, C. L.; Tamouza, S.; Passarello, J. P.; Tobaly, P.; De Hemptinne, J. C. Modeling phase equilibrium of H<sub>2</sub> + *n*-alkane and CO<sub>2</sub> + *n*-alkane binary mixtures using a group contribution statistical association fluid theory equation of state (GC-SAFT-EOS) with a *kij*

group contribution method. *Ind. Eng. Chem. Res.* **2006**, 45 (20), 6803–6810.

(23) Tang, X.; Gross, J. Modeling the phase equilibria of hydrogen sulfide and carbon dioxide in mixture with hydrocarbons and water using the PCP-SAFT equation of state. *Fluid Phase Equilib.* **2010**, 293, 11–21.

(24) D'Souza, R.; Patrick, J. R.; Teja, A. S. High pressure phase equilibria in the carbon dioxide–*n*-hexadecane and carbon dioxide–water systems. *Can. J. Chem. Eng.* **1988**, 66 (2), 319–323.

(25) Hölscher, I. F.; Spee, M.; Schneider, G. M. Fluid-phase equilibria of binary and ternary mixtures of CO<sub>2</sub> with hexadecane, 1-dodecanol, 1-hexadecanol, and 2-ethoxy-ethanol at 333.2 and 393.2 K and at pressures up to 33 MPa. *Fluid Phase Equilib.* **1989**, 49, 103–113.

(26) Huie, N. C.; Luks, K. D.; Kohn, J. P. Phase-equilibria behavior of systems carbon dioxide–*n*-eicosane and carbon dioxide–*n*-decane–*n*-eicosane. *J. Chem. Eng. Data* **1973**, 18 (3), 311–313.

(27) Sato, Y.; Tagashira, Y.; Maruyama, D.; Takishima, S.; Masuoka, H. Solubility of carbon dioxide in eicosane, docosane, tetracosane, and octacosane at temperatures from 323 to 473 K and pressures up to 40 MPa. *Fluid Phase Equilib.* **1998**, 147 (1–2), 181–193.

(28) Kordikowski, A.; Schneider, G. M. Fluid phase equilibria of binary and ternary mixtures of supercritical carbon dioxide with low-volatility organic substances up to 100 MPa and 393 K. *Fluid Phase Equilib.* **1993**, 90 (1), 149–162.

(29) Gau, C.-Y.; Stadtherr, M. A. Deterministic global optimization for error-in-variables parameter estimation. *AIChE J.* **2002**, 48 (6), 1192–1197.

(30) Mraw, S. C.; Hwang, S.-C.; Kobayashi, R. Vapor–liquid equilibrium of the methane–carbon dioxide system at low temperatures. *J. Chem. Eng. Data* **1978**, 23 (2), 135–139.

(31) Al-Sahhaf, T. A.; Kidnay, A. J.; Sloan, E. D. Liquid + vapor equilibria in the nitrogen + carbon dioxide + methane system. *Ind. Eng. Chem. Fundam.* **1983**, 22 (4), 372–380.

(32) Horstmann, S.; Fischer, K.; Gmehling, J.; Kolár, P. Experimental determination of the critical line for (carbon dioxide + ethane) and calculation of various thermodynamic properties for (carbon dioxide + *n*-alkane) using the PSRK model. *J. Chem. Thermodyn.* **2000**, 32 (4), 451–464.

(33) Smejkal, Q.; Martin, A.; Kerler, B. Thermodynamic data of CO<sub>2</sub>-rich multi-component systems: Opalescence measurements versus ASPEN PLUS computer simulation. *J. Supercrit. Fluids* **2002**, 24 (3), 183–192.

(34) Hsu, J. J. C.; Nagarajan, N.; Robinson, R. L. Equilibrium phase compositions, phase densities, and interfacial tensions for carbon dioxide + hydrocarbon systems. 1. Carbon dioxide + *n*-butane. *J. Chem. Eng. Data* **1985**, 30 (4), 485–491.

(35) Liu, J.; Qin, Z.; Wang, G.; Hou, X.; Wang, J. Critical properties of binary and ternary mixtures of hexane + methanol, hexane + carbon dioxide, methanol + carbon dioxide, and hexane + carbon dioxide + methanol. *J. Chem. Eng. Data* **2003**, 48 (6), 1610–1613.

(36) Choi, E.-J.; Yeo, S.-D. Critical Properties for Carbon Dioxide + *n*-Alkane Mixtures Using a Variable-Volume View Cell. *J. Chem. Eng. Data* **1998**, 43 (5), 714–716.

(37) Reamer, H. H.; Sage, B. H. Phase equilibria in hydrocarbon systems. Volumetric and phase behavior of the *n*-decane–CO<sub>2</sub> system. *J. Chem. Eng. Data* **1963**, 8 (4), 508–513.

(38) Enick, R.; Holder, G. D.; Morsi, B. I. Critical and three phase behavior in the carbon dioxide/tridecane system. *Fluid Phase Equilib.* **1985**, 22 (2), 209–224.

(39) Scheidgen, A. Fluidphasengleichgewichte binärer und ternärer Kohlendioxidmischungen mit schwerflüchtigen organischen Substanzen bis 100 MPa. Cosolvency effekt, mischbarkeit fenster, und Löcher in der kritischen Fläche. Dissertation, Ruhr-Universität Bochum, Bochum, Germany, 1997.

(40) Spee, M.; Schneider, G. M. Fluid phase equilibrium studies on binary and ternary mixtures of carbon dioxide with hexadecane, 1-dodecanol, 1,8-octanediol, and dotriacontane at 393.2 K and at pressures up to 100 MPa. *Fluid Phase Equilib.* **1991**, 65, 263–274.

(41) Hottovy, J. D.; Kohn, J. P.; Luks, K. D. Partial miscibility behavior of the ternary systems methane–propane–*n*-octane, methane–*n*-butane–*n*-octane, and methane–carbon dioxide–*n*-octane. *J. Chem. Eng. Data* **1982**, 27 (3), 298–302.

(42) Kukarni, A. A.; Zarah, B. Y.; Luks, K. D.; Kohn, J. P. Phase-equilibria behavior of system carbon dioxide–*n*-decane at low temperatures. *J. Chem. Eng. Data* **1974**, 19 (1), 92–94.

(43) Hottovy, J. D.; Luks, K. D.; Kohn, J. P. Three-phase liquid–liquid–vapor equilibria behavior of certain binary carbon dioxide–*n*-paraffin systems. *J. Chem. Eng. Data* **1981**, 26 (3), 256–258.

(44) van der Steen, J.; de Loos, T. W.; de Swaan Arons, J. The volumetric analysis and prediction of liquid–liquid–vapor equilibria in certain carbon dioxide + *n*-alkane systems. *Fluid Phase Equilib.* **1989**, 51, 353–367.

(45) Fall, D. J.; Fall, J. L.; Luks, K. D. Liquid–liquid–vapor immiscibility limits in carbon dioxide + *n*-paraffin mixtures. *J. Chem. Eng. Data* **1985**, 30 (1), 82–88.